2020-03

Developing a stochastic model for studying and simulating sediment transport in ports and harbors

Msamba, Oscar Menrad

NM-AIST

DEVELOPING A STOCHASTIC MODEL FOR STUDYING AND SIMULATING SEDIMENT TRANSPORT IN PORTS AND HARBORS

Oscar Menrad Msamba

A Dissertation Submitted in Partial Fulfilment of the Requirements for the Degree of Master's in Mathematical and Computer Sciences and Engineering of the Nelson Mandela African Institution of Science and Technology

Arusha, Tanzania

March, 2020

ABSTRACT

A particle model for describing and predicting sediment transport in shallow water is developed with the use of random walk models by showing consistency between the Fokker-Plank equation and the Advection diffusion equations. In the model, erosion and deposition processes are developed probabilistically where by the erosion term is considered to be a constant and deposition term is taken as a function by relating sediment settling velocity and diffusion coefficient. The model was simulated by considering three environment tests. In each environment test, the simulations show the distribution of each particle at any given time t. They also show the particles that will finally remain in suspension state and the particles that will be deposited during the transport process following the deployment of 10 000 particles. It was established that there is uniform distribution of particles in test environment I and III and a linear dependence between the number of particles in different grid cell and the water depth in test environment II.

DECLARATION

I, Oscar Menrad Msamba, do hereby declare to the Senate of Nelson Mandela African Institution of Science and Technology that this dissertation is my own original work and that it has neither been submitted nor presented for similar a award in any other institution.

Oscar Menrad Msamba (Candidate)	Date

The above declaration is confirmed

Prof. Verdiana Grace Masanja (Supervisor 1)	Date
Dr. Wilson Charles Mahera (Supervisor 2)	Date

COPYRIGHT

CERTIFICATION

The undersigned certify that they have read and hereby recommend for acceptance by the Nelson Mandela African Institution of Science and Technology the dissertation entitled: Developing a Stochastic Model for Studying and Simulating Sediment Transpot in Ports and Harbours, in fulfillment of the requirements for the degree of Masters in Mathematical and Computer Sciences and Engineering of the Nelson Mandela African Institution of Science and Technology.

Prof. Verdiana Grace Masanja
(Supervisor 1)

Date: .....

Dr. Wilson Charles Mahera
(Supervisor 2)

Date: .....

ACKNOWLEDGEMENT

It is my pleasure to acknowledge the following for their outstanding support in preparation of this dissertation. First and foremost, with many thanks, I express my sincere appreciations to my supervisors, Prof. Verdiana Grace Masanja and Dr. Wilson Charles Mahera for their support, guidance and encouragement on how to go about in this research work through discussions and meetings. Without their support, this dissertation would have been impossible. I also like to submit my thanks to my employer Arusha Technical College and General Studies Department for their trust to release me to pursue my studies. I also submit my thanks to my sponsor African Development Bank (AfDB) for their financial support, sincerely without their support, I could not have chance to pursue my studies. I also acknowledge the benefit I received from generosity of many people and special thanks should go to the following. Mr.Stefan de Gijsel(TU delft University), Mr. Shija Mbitila(Arusha Technical College), and Mr. Omari Mzava (Arusha Technical College) who provided MATLAB support on model simulation and Mr.Ramadhan Issa (Arusha Technical College) who edited this dissertation. Lastly but not least, I would like to submit my thanks to my parents, sisters and brothers for their physical and emotional care. I also indebted to thank the whole community of NM-AIST for their support during my studies.

DEDICATION

I dedicate this work to my parents and friends.

TABLE OF CONTENTS

LIST OF TABLES

LIST OF FIGURES

LIST OF APPENDICES

LIST OF ABBREVIATIONS AND SYMBOLS

PDF	Probability Density Function
FPE	Fokker-Plank Equation
ODEs	Ordinary Differential Equations
ODE	Ordinary Differential Equation
NM-AIST	The Nelson Mandela Institution of Science and Technology
SDEs	Stochastic Differential Equations
SDE	Stochastic Differential Equation
PTM	Particle Tracking Model
COCSE	Communication and Computational Science and Engineering

CHAPTER ONE

INTRODUCTION

1.1 Background of the problem

Sediment transport deals with movement of fragmented materials (particles) by flowing water. There are three types of sediment transport: bedload, saltation and suspension. Bedload transport involves the movement of sediment grain along the bed. Saltation involves jumping of a single grain whose length is proportional to its diameter over the bed. Suspension occurs when the flux is enough to move a sediment particle to a considerable height over the bed. These variations in particle movement are caused by a number of factors namely: variation of particle properties such as size, shape, mass or contents, and force exerted on the particle where by low force results to insufficient velocity of the particle which cause deposition while high force results to sufficient velocity of the particle to cause erosion. When sediment transport is turbulent in nature, the randomness results to variations in particles movement. In extreme flows, sediment transport has a number of negative impacts: reduction in water depth in ports and harbours, environmental damages, poor water quality, destruction of land resources and structures, and economic losses.

Since the accumulation of sediments in harbours and ports continues to be a challenge in ports planning and operations as it leads to reduced water depth which hinders large ships to dock Sanga and Dubi (2004), there is a need of a clear understanding of sediment transport rate to control effects associated with sediment transport. This study focuses on developing a stochastic model for studying and simulating sediment transport in ports and harbors that can be used to predict the transportation rate of sediments and change in water depths. Thus, before planning and executing dredging activities there is a need for understanding sedimentation rates. High rates of sedimentation bring the necessity of frequent dredging, this bring high-cost implication to ports and harbours operations.

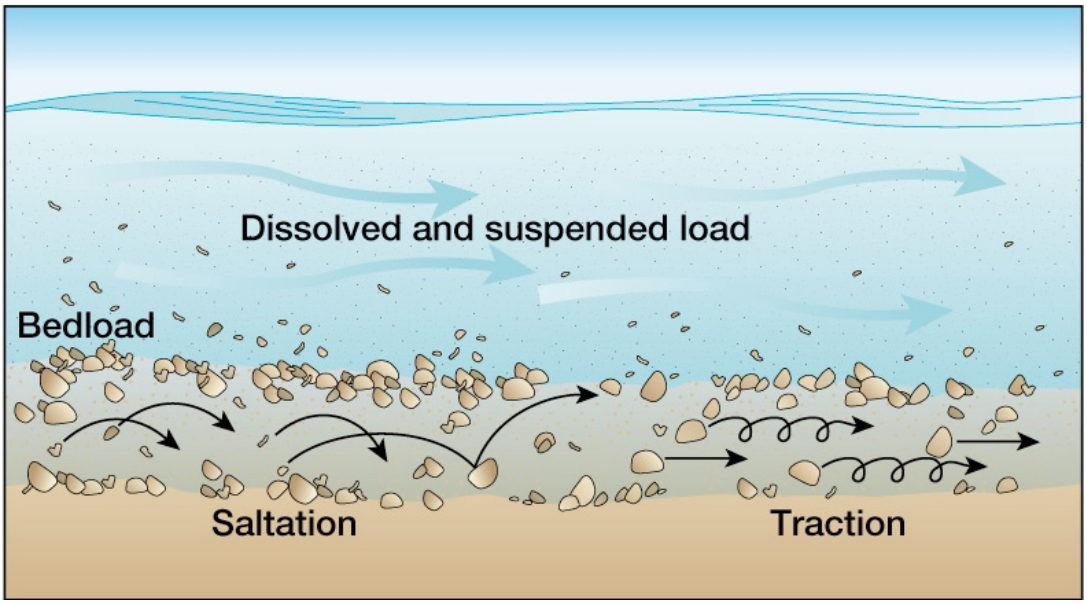

Figure 1: Types of sediment transport

1.1.1 Sediments classification

Sediment particles can be described as cohesive or non-cohesive, although both of the two have; diameter, density and porosity. Cohesive sediment are defined to be those particles with organic matter in a large content or clays. Its electromagnetic property cause the particles binding together, this type of sediment includes; clay, silt and other organic matter with gelatinous property. Contrary to cohesive, non-cohesive sediments have no electromagnetic property and usually made up by medium and fine grade sands. According to American Geophysical Union soil can be classified according to size as shown in Table 1 Union (1957).

Table 1: American Geophysical Union sediment classification system

Type of sediment particle	Scaling	Non-cohesive	Diameter in millimeters
Clay	Very fine	No	0.0005-0.00024
	Fine	No	0.00010-0.0005
	Medium	No	0.002-0.001
	Coarse	No	0.004-0.002
Silt	Very fine	Yes	0.008-0.004
	Fine	Yes	0.016-0.008
	Medium	Yes	0.031-0.016
	Coarse	Yes	0.062-0.031
Sand	Very fine	Yes	0.125-0.062
	Fine	Yes	0.25-0.125
	Medium	Yes	0.5-0.25
	Coarse	Yes	1.0-0.5
	Very coarse	Yes	2-1
Gravel	Very fine	Yes	4-2
	Fine	Yes	8-4
	Medium	Yes	16-8
	Coarse	Yes	32-16
	Very coarse	Yes	64-32

Particle size is of paramount important characteristics when one wants to describe sediment transport. This property affects; deposition, erosion and transport rates. As it is used in this study, many models use the diameter (d) and the approximation d_{50} is used in sediments classification as it is shown in Table 1.

Clay is described as granular material and made from feldspar and mineral quartz and often it is in spherical shape. Based on the Udden-Wentworth scale, the size scale of clay may overlap with silt.

Silt represents very fine graded natural rock made of clay minerals, organic matters and metal oxides. Because of this composition, it is considered to have cohesive properties and due to electromagnetic forces silt are very sticky.

Sand consists of granular material formed by mineral particles or finely divided rock. It con-

tains calcium carbonate or silica (quartz). Grading down of gravel and other large particles results to sand which ranges from 2 mm to 0.062 mm as shown in Table 1. Particles of newer sand and older sand are described to be irregular and spherical in shape respectivey.

Gravel consists of unconsolidated rock fragments which have been smoothed or not by the flowing water. It can be graded into various types from very fine at $2-4$ mm, as presented in Table 1. Gravel has a density approximatelly 1800 kg/m^3.

1.2 Statement of the problem

There are a number of extensive researches that have been done on sediment transport mechanics and came up with mathematical models to predict the rate of sedimentation. These researches includes: Bijker (1980), Rijn (1986), Bakker (2009), Herrera-Díaz *et al.* (2017), Knaapen and Wertwijn (2013) and Mahera and Narsis (2013),

Most of these studies have developed simplified stochastic models which neglect parameters of the uncertainties. However, the uncertainties are very essential for accurate prediction of sediment transport rate. In this study, advanced stochastic methods that incorporate necessary uncertainties for accurate predictions will be used to develop a stochastic model for studying and simulating sediment transport in ports and harbours.

1.3 Objectives

1.3.1 General objective

The general objective of this study is to develop a stochastic model for studying and simulating sediment transport in ports and harbours based on advanced stochastic methods.

1.3.2 Specific objectives

The specific objectives of the study were to:

(i) Develop a stochastic model that include uncertainties and use it for studying and simulating sediment transport in ports and harbours.

(ii) Simulate the model to predict scenarios that can be used by management to mitigate the challenges caused by reduced water depth in ports and harbours.

(iii) Compare the modified model with other stochastic models without erosion and deposition terms.

1.4 Significance of the research study

This research study is certainly significant due to the following reasons:

(i) It will provide a comprehensive analysis of the probabilistic properties of sediment transport in ports and harbours. This will assist port and harbour engineers with more knowledge on sediment transport dynamics in ports and harbours.

(ii) It will provide researchers with new knowledge on the application of new advanced stochastic techniques for predicting sediment transport. This will also help them to account for uncertainties associated with sediment transport in ports and harbours.

(iii) It will provide important details needed by engineers to design harbours and ports which are less prone to reduced water depths by enabling accurate simulations.

CHAPTER TWO

LITERATURE REVIEW

This chapter includes four sections, each section discusses the concepts in which this thesis is build upon. The first section discusses the deterministic method as one way of describing sediment transport. The second section discusses the stochastic method to describe sediment transport and various research studies that have been done on sediment transport to present. It also discusses other methods for describing sediment transport such as Particle Tracking Methods (PTMs) and other important concepts which are important in Stochastic modelling. The third section explains about advection diffusion process and the fourth section discusses the numerical schemes that can be used to solve Stochastic Differential Equations (SDEs).

2.1 Deterministic methods

Deterministic model uses mathematical relationships based on the principles of biology, physics and chemistry such as conservation of mass and momentum principle to simulate a certain physical phenomenon without considering entirely the effect of variable uncertainties.There are number of numerical models developed so far to describe sediment transport in deterministic form. Some developed models for bedload transport and others for suspended load transport. Bedload transport occurs when sediment particles rolls or slide along the streambed while sediment transport in suspension form is much influenced mean flow of water turbulence Dade and Friend (1998). Deterministic differential equation was employed by different authors such as Amoudry and Souza (2011) and Senior *et al.* (2003) to develop deterministic models for estimating sediment concentration or fluxes. It can also be used to supply uncertainty information if hybrid approach is used in the sense that stochastic parameters are introduced to the model.

2.2 Stochastic methods

Understanding sediment transport process is still a continuing challenge to engineers and scientist as the process is influenced by many uncertainties which must be considered so as to have accurate prediction of sediment transport. Stochastic modelling idea becomes more significant than deterministic in engineering fields as it attaches parameters of uncertainty associated with sediment transport process. Usually it describes the statistical pattern of a certain phenomenon to show randomness. The idea of analysing sediment transport was first initiated by Einstein

(1937, 1950) and Kalinske (1947). The idea was the extended by Li and Shen (1975) and Hung and Shen (1976)

Bijker (1980) developed a simple mathematical model for sediment transport rate by schematizing the transport process. The model depends on the availability of dredge results to calibrate the empirical coefficients or when the rough estimate of sediment is considered to be adequate.

Rijn (1986) developed a two-dimensional vertical model for sedimentation of dredged channel. Unlike the traditional formulas which based on strong schematization of the transport process, this model developed on the basis of representation of the relevant transport processes such as mixing, settling, and convection. It investigated the effects of current and wave on sedimentation of the suspended transport. This model also depends much on the presence of waves and currents boundary conditions, when there is no detailed information about boundary condition the model cannot be used to provide an accurate estimation of sediment transport rate.

Bakker (2009) developed a simplified stochastic model for estimating channel infill and providing an overview of the effects of sediment transport uncertainties in estimating sedimentation rate. The study considered three important uncertainties in the sedimentation process, these uncertainties include, the effect of currents, the effect of waves and the effect of sedimentation concentration. The model developed depends much on the site information (data), so accurate measurement of necessary data is needed if one wishes to employ this method. Thus, when the current climate, weather climate, and sediment characteristics are well investigated the method can be efficiently applied.

Knaapen and Wertwijn (2013) developed a mathematical model based on a probabilistic approach by considering the impact of uncertainties in sediment composition and the bed structure. As in practice, it is difficult to get the precise information on sediment and the bottom characteristics the authors used ensemble simulation to predict sedimentation rate under the uncertainties of sediment composition and bed structure. This model ignores other uncertainties like in flow, water level and wave condition, however in many cases, these are the main uncertainties in sedimentation of ports and harbours.

Mahera and Narsis (2013) developed a particle model in two-dimensional for sediment transport by adding two important terms: deposition and erosion . This model considered deposition and erosion terms as constants.

Herrera-Díaz *et al.* (2017) developed a light particle tracking model for simulating the bed sediment transport load. The model developed tries to determine if the erosion, deposition and

sediment concentration are governed by the probabilistic function by considering the number of particles and size contained in every cell. The model also is based on the simplification, for instance, the authors considered the horizontal scale is larger than the vertical scale. The developed model is useful for validation of the sediment transport model developed specifically to obtain results in a short time period.

2.2.1 Wiener process

According to Campolieti and Makarov (2018), a Wiener continuous stochastic process $\{W(t)\}_{t\geq 0}$ is defined to be Gaussian on the sample space $(\Omega, \mathscr{F}, P)$ if it satisfies the following properties

(i) $W(0) = 0$, that is almost each path has the starting point at the origin with the probability one.

(ii) for $n \in N$ and every choice of the partition $0 \leq t_0 < t_1 < ...t_n$, the increments$W(t_1) \equiv W(t_1) - W(t_0), W(t_2) - W(t_1)...W(t_n) - W(t_{n-1})$ are independent. In other words non-overlaping increments are jointly independent.

(iii) For arbitrary t and $0 \leq s < t$, the increment $W(t+\Delta t) - W(t)$ is normally distributed with mean 0 and variance Δt i.e $\Delta W(t) \sim N[0, \Delta t]$

A continuous stochastic Wiener process is called a standard Brownian Motion with the following properties

(i) $W(0) = 0$ with the probability one

(ii) (Non overlaping increments are independent) for any $n\varepsilon N$ in $0 \leq t_0 < t_1 < ...t_n$, the increments $W(t_1) - W(t_0), W(t_2) - W(t_1)...W(t_n) - W(t_{n-1})$ are independent

(iii) For all $0 \leq s < t$, $W(t) - W(s)$ has a normal distribution with mean 0 and variance $t - s$;

$$E[W(t) - W(s)] = 0, Var[W(t) - W(s)] = t - s, W(t) - W(s) \sim N(0, t - s)$$

(iv) For all $w \in \Omega$, the path $W(t, w)$ is continuous.

According to Higham (2001), it is very important to put into consideration a discretized Brownian version of motion for computational purposes, where a continuous Wiener stochastic process $\{W(t)\}_{t\geq 0}$ is specified at discrete t values, thus by setting $\delta t = \dfrac{T}{N}$ and for some positive

integer N and let W_n denote $W(t_n)$ with $t_n = n\delta t$. Thus with condition 1, 2 and 3 of Brownian motion, $W_0 = 0$ with probability 1 and $W_n = W_{n-1} + dW_n$, for $n = 1, 2, ...N$, where every dW_n is an independent random variable of the form $\sqrt{\delta t}N[0,1]$.

The following plot demonstrate the simulation Brownian motion discretized in $[0,1]$ when $N = 700$. In this simulation the random number generator was used to gerate random numbers in $N[0,1]$ and the code for Fig. 2 was written by Higham (2001).

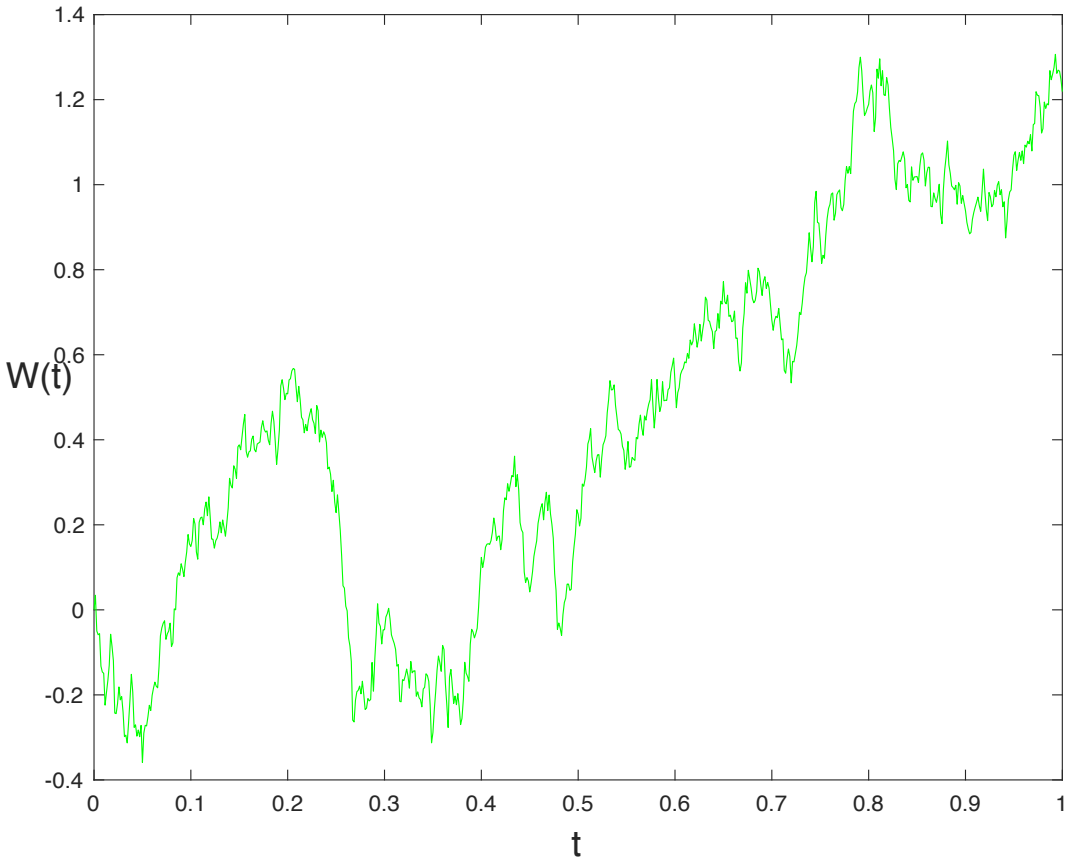

Figure 2: Discretized Brownian path

2.2.2 Particle tracking model

Many studies use Particle Tracking Model (PTMs) to describe movement of individual particle in water flow. PTMs uses either or both Langragian and Eulerian approach(es). For example, in ground water modelling, earlier researchers such as Prickett *et al.* (1981) have used PTMs by considering the mean flow velocity. Uffink (1983), Dimou and Adams (1993) published by putting into consideration the drift term because of variation of the dispersion coefficient.

The governing equation of many recent works on PTMs use two terms which are random term because of turbulence nature and drift term because of mean flow, these terms show stochastic and deterministic movement of a particle respectively.

Consider the following physical system $X(t)$ described by the following ordinary differential equation with the initial condition $X(t_0) = x(0)$

$$\frac{dx}{dt} = f(x,t). \tag{2.1}$$

The following is the integral form of differential equation (2.1):

$$X(t) = X(0) + \int_{t_0}^{t} f(X(s),s)ds. \tag{2.2}$$

By adding uncertainty in the Ordinary differential equation (2.1) with the solution $X(t) = X(t|x_0,t_0)$, the equation becomes SDE which is the following Equation (2.3).

$$\frac{dX(t)}{dt} = f(X(t),t) + g(X(t),t)\xi(t), X(t_0) = x_0. \tag{2.3}$$

The term $\xi(t)$ is the added stochastic process to make the deterministic differential equation SDEs. Initial condition of the SDEs must also be random variable. The Equation (2.3) (2.3) is continuous, to be a Markov it should be discretized, that is the probability that $X_n = j$ should depend on the present state of the system. In other words to determine the future state of the system there is no need of information at each step rather than the present information. Mathematically this is presented by Equation (2.4).

$$Pr\{X_n = j|X_{n-1} = i\}, \tag{2.4}$$

This means that $X_n = j$ given that $X_{n-1} = i$, the probability does not depend on the states $X_{n-2}, X_{n-3}...X_1$. More information about Markovian process is contained in Øksendal (2003).

2.2.3 Stochastic differential equations

According to Campolieti and Makarov (2018), the stochastic differential equation can be written in general form as:

$$dX_i(t) = \mu_i(t,X(t))dt + \sum_{j=1}^{d} \sigma_{ij}(t,X(t))dW_j(t), i = 1,2,...n, \tag{2.5}$$

The integral form of equation (2.5) is:

$$X_i(t) = X_i(0) + \int_0^t \mu_i(s,X(s))ds + \sum_{j=1}^{d} \int_0^t \sigma_{ij}(s,X(s))dW_j(s), i = 1,2,3...n. \tag{2.6}$$

Whre $\mu_i(t,X(t))$ is the drift(deterministic) term and $\sigma_{ij}(t,x)$ is the stochastic term. Both of the terms are the functions of time and variable X, $(X_1,X_2,X_3...X_i(t))^T$ stands for the particle location (position), $dW_j(t)$ stands for the Wiener increment, and according to Section (2.2.1) it has the following properties.

$$E[dW_j(t)] = 0, \tag{2.7}$$

$$E[dW_i(t_1)dW_j(t_2)] = \begin{cases} 0 \text{ if i} \neq \text{j or } t_1 = t_2 \\ dt_1 \text{ if i=j and } t_1 = t_2. \end{cases} \tag{2.8}$$

To find solution of the SDEs (2.5), consider the following SDEs (2.9) reduced to one dimensional defined on $0 \leq t_0 \leq t \leq \infty$.

$$dX(t) = \mu(X(t),t)dt + \sigma(t,X(t))dW(t), X(t_0) = x_0. \tag{2.9}$$

The integral form of equation (2.9) is:

$$X(t) = X(t_0) + \int_{t_0}^{t} \mu(X(s),s)ds + \int_{t_0}^{t} \sigma(X(s),s)dW(s). \tag{2.10}$$

2.2.4 Stochastic integral

To solve the SDEs (2.9) one need to be careful as it contains both Riemman integral and stochastic integral which are represented by first and second integrals on the right handside of equation (2.10). When $\sigma = 0$, the equation (2.9) becomes similar to ordinary differential equation. Therefore to approximate the solution of the SDEs (2.9) the knowledge to evaluate the following stochastic integral (2.11) is needed.

$$\int_{t_0}^{t} \sigma(X(s),s)dW(s). \tag{2.11}$$

The integral (2.11) above can be solved by using Stratonovich or an *Itô* formula by considering the position of the function $\sigma(X(s),s)$. More discussion on *Itô* and Stratonovich is contained in subsection (2.2.5) and in the following literatures Øksendal (2003) and Milstein (1994).

2.2.5 *Itô* and Stratonovich integrals

To solve equation (2.11), consider the following Riemman Stieltjes sum (2.12):

$$S_n = \sum_{i=1}^{n} W(t_{i-1})(W(t_i) - W(t_{i-1})). \tag{2.12}$$

By using the intermediate nodes $S_i = t_{i-1}$ for each $i = 1,2,...n$ and the identity $a(b-a) = \frac{1}{2}(a-b)^2 + \frac{1}{2}(b^2-a^2)$, the Riemman sum can be written as in the following equation (2.13):

$$S_n = -\frac{1}{2}\sum_{i=1}^{n}((W(t_i) - W(t_{i-1}))^2 - (W^2(t_i) - W^2(t_{i-1})), \tag{2.13}$$

$$S_n = -\frac{1}{2}\sum_{i=1}^{n}(W(t_i) - W(t_{i-1})^2 + \frac{1}{2}\sum_{i=1}^{n}(W^2(t_i) - W^2(t_{i-1}).$$

As $n \to \infty$ and $\sigma(P_n) \to 0$, then $\sum_{i=1}^{n}(W(t_i) - W(t_{i-1}))^2 \to [W,W](T) = T$ which is the Quadratic Variation of Brownian motion. Thus:

$$\lim_{n\to\infty} S_n = \frac{1}{2}(W^2(T) - W^2(0)) - \frac{T}{2}. \tag{2.14}$$

The limit represented by equation (2.14) is called *Itô* integral of Brownian motion Campolieti and Makarov (2018) and hence the approxiamate of stochastic integral can be found by using equation (2.15):

$$\int_{t_0}^{t} W(t)dW(t) = \frac{1}{2}(W^2(T) - W^2(0)) - \frac{T}{2}, \tag{2.15}$$

$$\int_{t_0}^{t} W(t)dW(t) = \frac{1}{2}(W^2(T) - T).$$

A different approach towards the derivation of *Itô* integral is to consider the intermediate partition $S_i = t_i$ with the upper end point for each $i = 1,2,...n$ the Riemman Stieljet sum becomes:

$$S_n^* = \sum_{i=1}^{n} W(t_i)(W(t_i) - W(t_{i-1})), \tag{2.16}$$

$$= \frac{1}{2}\sum_{i=1}^{n}(W(t_i) - W(t_{i-1}))^2 + \frac{1}{2}\sum_{i=1}^{n}(W^2(t_i) - W(t_{i-1})^2).$$

As $n \to \infty$ then $[W,W](T) = T$ and hence:

$$S_n^* = \frac{1}{2}(W^2(T) - W^2(0)) + \frac{T}{2}. \tag{2.17}$$

For $0 \leq \alpha \leq 1$, consider a weighted average of $0 \leq \alpha \leq 1$ and S_n^* equation (2.18) is obtained.

$$\alpha S_n + (1-\alpha)S_n^* = \sum_{i=1}^{n} (\alpha W(t_{i-1}) + (1-\alpha)W(t_i))(W(t_i) - W(t_{i-1})), \tag{2.18}$$

$$= \frac{1}{2}(W^2(T) - W^2(0)) + \frac{T}{2} - \alpha T.$$

As $n \to \infty$ and by considering the midpoint $\alpha = \frac{1}{2}$, the following interesting case of the limit is obtained which is called Stratonovich integral of Brownian motion.

$$\int_0^T W(t) \circ dW(t) = \frac{1}{2}(W^2(T) - W^2(0)). \tag{2.19}$$

The stratonovich integral applies even to non-stochastic ordinary calculus like integration by parts and chain rule Campolieti and Makarov (2018).

2.2.6 Kolmogorov forward equation in one dimension

Suppose that $X(t)$ represents the solution of Equation (2.9) with the transition probability density function $f(s,y;t,x)$, then under fairly general condition the PDF $f(s,y;t,x)$ satisfies the forward kolmogorov equation which is commonly known as Fokker-Planck equation.

$$\frac{d}{dt} f(s,y;t,x) = \varsigma f(s,y;t,x) \varepsilon(0,T) \times \mathbb{R}, \tag{2.20}$$

$$f(s,y;t,x) \to \delta y \text{as } s \; t \downarrow s,$$

Where:

$$\tilde{\varsigma} = -\frac{\partial}{\partial x}[\mu(x,t)] + \frac{1}{2}\frac{\partial^2}{\partial x^2}[\sigma^2(x,t)].$$

In compact form the equation (2.20) can be written as:

$$\frac{df}{dt} = \tilde{\varsigma} f, \tag{2.21}$$

$$dX(t) \overset{Itô}{=} \mu(X(t),t)dt + \sigma(X(t),t)dW(t), X(t_0) = x_0. \tag{2.22}$$

Consider the points S and T in time where $S < T$ and the test function $\Psi(x,t)$ having compact support on $(S,T) \times \mathbb{R}$ Björk (2009). Using $Itô$ formula equation (2.23) is obtained:

$$\Psi(X(T),T) = \Psi(X(s),s) + \int_s^T (\frac{\partial \Psi}{\partial t} + \tilde{\varsigma}\Psi)(X(t),t)dt + \int_s^T (\frac{\partial \Psi}{\partial x})(X(t),t)dW(t), \tag{2.23}$$

Where:

$$\tilde{\varsigma} = \frac{\partial}{\partial x}[\mu(x,t)] + \frac{1}{2}\frac{\partial^2}{\partial x^2}[\sigma^2(x,t)].$$

By using the expectation operator $E_{s,y}[.]$, to Equation (2.23) with the fact that $\Psi(x,T) = \Psi(x,s) = 0$, the following equation (2.24) is obtained.

$$E_{s,y}[\Psi(X(T),T) - \Psi(X(s),s)] = E_{s,y}\left[\int_s^T (\frac{\partial \Psi}{\partial t} + \tilde{\varsigma}\Psi)(X(t),t)dt\right] + E_{s,y}\left[\int_s^T \frac{\partial \Psi}{\partial x}(X(t),t)dW(t)\right], \tag{2.24}$$

$$0 = E_{s,y}\left[\int_s^T (\frac{\partial \Psi}{\partial t} + \tilde{\varsigma}\Psi)(X(t),t)\right]dt + 0,$$

$$E_{s,y}\left[\int_s^T (\frac{\partial \Psi}{\partial t} + \tilde{\varsigma}\Psi)(X(t),t)\right]dt = 0,$$

Hence:

$$\int_{-\infty}^{\infty}\int_s^T \left((\frac{\partial}{\partial t} + \tilde{\varsigma})\Psi(t,x)f(s,y;t,x)\right)dxdt = 0. \tag{2.25}$$

Applying partial integration to equation (2.25) that is integrating $\frac{\partial}{\partial t}$ with respect to t and $\tilde{\varsigma}$ with respect to x.

$$\int f(s,y;t,x)\Psi(x,t)dt = -\int \Psi(x,t)\frac{\partial}{\partial t}[f(s,y;t,x)]dt,$$

$$\int f(s,y;t,x)\mu(x,t)\Psi'(x,t)dx = -\int \Psi(x,t)\frac{\partial}{\partial x}[\mu(x,t)p(s,y;t,x)]dx,$$

$$\int f(s,y;t,x)\sigma^2(x,t)\Psi''(x,t)dx = \int \Psi(x,t)\frac{\partial^2}{\partial x^2}[\sigma^2(x,t)f(s,y;t,x)]dx,$$

As $x \to \infty$ and $x \to -\infty$ then $f(s,y;t,x) \to 0$ and hence:

$$E_{s,y}[\int_s^T (\frac{\partial \Psi}{\partial t} + \tilde{\varsigma}\Psi)(X(t),t)dt] = \int_{-\infty}^{\infty}\int_s^T \Psi(x,t)\{\frac{-\partial f(s,y;t,x)}{\partial t} + \tilde{\varsigma}^* f(s,y;t,x)\}dxdt,$$

$$\int_{-\infty}^{\infty}\int_s^T \Psi(x,t)(\frac{-\partial}{\partial t} + \tilde{\varsigma}^*)f(s,y;t,x)dxdt = 0,$$

Where the used operator $\tilde{\varsigma}^*$ is defined as:

$$(\tilde{\varsigma}v)^* = \frac{-\partial}{\partial x}[\mu(x,t)v(x,t)] + \frac{1}{2}\frac{\partial^2}{\partial x^2}[\sigma^2(x,t),v(x,t)].$$

Hence the proof is complete since the equation satisfies all test functions. More discussions and similar proof for multi-dimensional *Itô* -FPE can be found in Björk (2009).

2.3 Advection diffusion process

Sediment particles movement can be caused by two factors which are advection and diffusion. Advection occurs when the particle are dragged along with water when water flows. In most cases the advection effect is observed when water flows with a high velocity. On the other hand water molecules can also affeect particles, consider the diffusion of ink drop in water where by the ink spreads slowly until it becomes evenly distributed regardless the effect of water velocity. The following equation (2.26) is called advection diffusion equation which describes sediment transport process in shallow water.

$$\frac{\partial HC}{\partial t} = -\sum_{i=1}^{2} \frac{\partial}{\partial x_i}(U_i HC) + \sum_{i=1}^{2}\sum_{j=1}^{2} \frac{\partial}{\partial x_i}(HD_{i,j}\frac{\partial C}{\partial x_j}) + S + Q. \tag{2.26}$$

Where: H stands for depth of water, C stands for concentration, U_i stands for horizontal flow velocity, $D_{i,j}$ stands for coefficient of dispersion, S and Q represent sink and source terms.

2.4 Numerical schemes derivation for SDEs

Numerical schemes for solving SDEs have no difference to schemes used to solve ODEs. Different schemes of SDEs can solve the same SDE depending on the interpretation of the problem. Therefore, there is a neeed of careful selection of the scheme in order to get the right approximate solution of the SDE. Derivation of SDEs schemes can be done through the use of free derivative schemes or Stochastic Taylor series expansion Jentzen and Kloeden (2011). In this work Stochastic Taylor series expansion is used.

2.4.1 Expansion of Stochastic Taylor series

The concept of expanding Stochastic Taylor series is built on the use of more terms of the Taylor series so that the order of conergence is high. Consider the following expansion of *Itô* SDE.

$$dX(t) \overset{Itô}{=} \mu(X(t),t)dt + \sigma(X(t),t)dW(t), X(t_0) = x_0, \tag{2.27}$$

With the solution:

$$X(t) \overset{Itô}{=} X(t_0) + \int_{t_0}^{t} \mu(s,X(s))ds + \int_{t_0}^{t} \sigma(s,X(s))dW(s). \tag{2.28}$$

Consider the smooth function $v(t,X(t))$ and with the use of SDE (2.27), the differential of the function $v(t,X(t))$ gives the following *Itô* formula:

$$d[v(t,X(t))] = \frac{\partial v}{\partial t}\mid_{t,X(t)} dt + \mu(t,X(t))\frac{\partial v}{\partial x}\mid_{t,X(t)} dt + \frac{1}{2}\sigma^2(t,X(t))\frac{\partial^2 v}{\partial x^2}\mid_{t,X(t)} dt + \sigma \mid_{t,X(t)} \frac{\partial v}{\partial x}.dW(t) + 0.dt, \quad (2.29)$$

$$d[v(t,X(t))] = [\frac{\partial v}{\partial t} + \mu(t,X(t))\frac{\partial v}{\partial x} + \frac{1}{2}\sigma^2(t,X(t))\frac{\partial^2 v}{\partial x^2}]dt + \sigma(t,X(t))\frac{\partial v}{\partial x}.dW(t), \quad (2.30)$$

$$dv = \xi^{\circ} v dt + \xi^{1} v dW(t),$$

Where ξ° and ξ^{1} are:

$$\xi^{\circ} = \frac{\partial}{\partial t} + \mu(t,X(t))\frac{\partial}{\partial x} + \frac{1}{2}\sigma^2(t,X(t))\frac{\partial^2}{\partial x^2},$$

$$\xi^{1} = \sigma(t,X(t))\frac{\partial}{\partial x}.$$

When the *Itô* formula is applied to equation (2.28) specifically to drift term $\mu(s,X(s))$, the following differential equation (2.31) is obtained.

$$d[\mu(s,X(s))] = \xi^{\circ}\mu ds + \xi^{1}\mu dW(s). \quad (2.31)$$

Writing equation (2.31) in integral form:

$$\mu(s,X(s)) = \mu(X(t_0),t_0) + \int_{t_0}^{s} \xi^{\circ}\mu dz + \int_{t_0}^{s} \xi^{1}\mu dW(z). \quad (2.32)$$

Similarly, by applying *Itô* formula to diffusion term $\sigma(s,X(s))$ the following equation (2.33) is obtained:

$$d(\sigma(s,X(s))) = \xi^{\circ}\sigma ds + \xi^{1}\sigma dW(s). \quad (2.33)$$

Whose solution is:

$$\sigma(s,X(s)) = \sigma(t_0,X(t_0)) + \int_{t_0}^{s} \xi^{\circ}\sigma dz + \int_{t_0}^{s} \xi^{1}\sigma dW(z). \quad (2.34)$$

By substituting equation (2.32) and (2.34) into (2.28) the following equation (2.35) is obtained:

$$X(t) = X(t_0) + \int_{t_0}^{t} \{\mu(t_0,X(t_0)) + \int_{t_0}^{t} \xi^{\circ}\mu(z,X(z))dz + \int_{t_0}^{s} \xi^{1}\mu(X(z),z)dW(z)\}ds + \int_{t_0}^{t} \{\sigma(t_0,X(t_0)) + \int_{t_0}^{t} \xi^{\circ}\sigma(z,X(z))dz + \int_{t_0}^{s} \xi^{1}\sigma(X(z),z)dW(z)\}dW(s), \quad (2.35)$$

$$X(t) = X(t_0) + \mu(t_0, X(t_0) \int_{t_0}^{t} ds + \sigma(t_0, X(t_0)) \int_{t_0}^{t} dW(s) + \int_{t_0}^{t}\int_{t_0}^{s} \tilde{\varsigma}^{\circ}\mu dz ds$$
$$+ \int_{t_0}^{t}\int_{t_0}^{s} \tilde{\varsigma}^{1}\mu dW(z) ds + \int_{t_0}^{t}\int_{t_0}^{s} \tilde{\varsigma}^{\circ}\sigma dz dW(s) + \int_{t_0}^{t}\int_{t_0}^{s} \tilde{\varsigma}^{1}\sigma dW(z) dW(s), \quad (2.36)$$

This lead to the first approximation:

$$X(t) = X(t_0) + \mu(t_0, X(t_0))(t - t_0) + \sigma(t_0, X(t_0))(W(t) - W(t_0)) + \int_{t_0}^{t}\int_{t_0}^{s} \tilde{\varsigma}^{\circ}\mu dz ds$$
$$+ \int_{t_0}^{t}\int_{t_0}^{s} \tilde{\varsigma}^{1}\mu dW(z) ds + \int_{t_0}^{t}\int_{t_0}^{s} \tilde{\varsigma}^{\circ}\sigma dW(s) ds + \int_{t_0}^{t}\int_{t_0}^{s} \tilde{\varsigma}^{1}\sigma dW(z) dW(s), \quad (2.37)$$

$$X(t) = X(t_0) + \mu(t_0, X(t_0))(t - t_0) + \sigma(t_0, X(t_0))(W(t) - W(t_0)) + Err_1, \quad (2.38)$$

$$X(t + \Delta t) = X(t) + \mu(t, X(t))\Delta t + \sigma(t, X(t))(W(t + \Delta t) - W(t)). \quad (2.39)$$

Or by using $t = n\Delta t$, the following Iteration equation is obtained.

$$X_{n+1} = X_n + \mu(t_n, X_n)\Delta t_n + \sigma(t_n, X_n)\Delta W(t_n). \quad (2.40)$$

From this derivation the functions $\mu(t, X(t))$ and $\sigma(t, X(t))$ are assumed to be sufficient smooth functions. Again the *Itô* rule applied to the terms of higher order in the integral of equation (2.37) so as to get the higher order convergence scheme. The first three terms of equation (2.37) led to the Stochastic Euler scheme where by:

$$Err_1 = \int_{t_0}^{t}\int_{t_0}^{s} \tilde{\varsigma}^{\circ}\mu dz ds + \int_{t_0}^{t}\int_{t_0}^{s} \tilde{\varsigma}^{1}\mu dW(z) ds + \int_{t_0}^{t}\int_{t_0}^{s} \tilde{\varsigma}^{\circ}\sigma dz dW(s) + \int_{t_0}^{t}\int_{t_0}^{s} \tilde{\varsigma}^{1}\sigma dW(z) dW(s). \quad (2.41)$$

By analyzing the next error term,the next error term with the lowest order of convergence can be obtained from equation (2.41).

$$\int_{t_0}^{t}\int_{t_0}^{s} \tilde{\varsigma}^{1}\sigma dW(z) dW(s). \quad (2.42)$$

Applying the *Itô* formula of differentiation to the function $\tilde{\varsigma}^{1}\sigma$ the following higher order approximation (2.43) is obtained:

$$d(\tilde{\varsigma}^{1}\sigma) = \tilde{\varsigma}^{\circ}\tilde{\varsigma}^{1}\sigma dz + \tilde{\varsigma}^{\circ}\tilde{\varsigma}^{1}\sigma dW(z). \quad (2.43)$$

The equation (2.43) above, can integrated as follows:

$$\xi^1\sigma(r,X(r)) = \xi^1\sigma(t_0,X(t_0)) + \int_{t_0}^{z} \xi^\circ\xi^1\sigma dr + \int_{t_0}^{z} \xi^\circ\xi^1\sigma dW(r). \tag{2.44}$$

Using equation (2.44) into (2.37) the following equation (2.45) is obtained:

$$\begin{aligned} X(t) = X(t_0) + \mu(t_0,X(t_0))(t-t_0) + \sigma(t_0,X(t_0))[W(t)-W(t_0)] \\ + \xi^1\sigma(t_0,X(t_0)) \int_{t_0}^{t}\int_{t_0}^{s} dW(z)dW(s) + Err_2. \end{aligned} \tag{2.45}$$

The result obtained gives a scheme with accuracy of higher order. The name of the scheme obtained is called Milstein scheme which is defined as:

$$\begin{aligned} X(t) = X(t_0) + \mu(t_0,X(t_0))(t-t_0) + \sigma(t_0,X(t_0))[W(t)-W(t_0)] \\ + \frac{1}{2}\sigma(t_0,X(t_0))\frac{\partial\sigma}{\partial x}\{(W(t)-W(t_0))^2 - (t-t_0)\} + Err_2, \end{aligned} \tag{2.46}$$

Where:

$$\begin{aligned} Err_2 = &\int_{t_0}^{t}\int_{t_0}^{s} \xi^\circ\mu(X(z),z)dzds + \int_{t_0}^{t}\int_{t_0}^{s} \xi^1\mu(z,X(z))dW(z)ds + \int_{t_0}^{t}\int_{t_0}^{s} \xi^\circ\sigma(z,X(z))dzdW(s) \\ &+ \int_{t_0}^{t}\int_{t_0}^{s}\int_{t_0}^{z} \xi^\circ\xi^1\sigma(r,X(r))drdW(z)dW(s) + \int_{t_0}^{t}\int_{t_0}^{s}\int_{t_0}^{z} \xi^\circ\xi^1\sigma(r,X(r))dW(r)dW(z)dW(s). \end{aligned} \tag{2.47}$$

Lets analyze the error term obtained in equation (2.46) as follows:

$$\int_{t_0}^{t}\int_{t_0}^{s} \xi^1\sigma(X(t_0),t_0)dW(z)dW(s) < K_4 \int_{t_0}^{t}\int_{t_0}^{s} dW(z)dW(s), \tag{2.48}$$

From this last Error term $K_4 = \xi^1\sigma(t_0,X(t_0))$ which is a constant.

$$\begin{aligned} K_4\int_{t_0}^{t}(W(s)-W(t_0))dW(s) &= K_4\{\int_{t_0}^{t} W(s)dW(s) - \int_{t_0}^{t} W(t_0)dW(s)\}, \\ &= K_4\{\frac{W^2(t)-W^2(t_0)}{2} - \frac{(t-t_0)}{2} - W(t_0)(W(t)-W(t_0))\}, \end{aligned} \tag{2.49}$$

$$K_4 \int_{t_0}^{t} (W(s) - W(t_0))dW(s) = K_4\{\int_{t_0}^{t} W(s)dW(s) - \int_{t_0}^{t} W(t_0)dW(s)\}, \tag{2.50}$$

$$\begin{aligned}
&= K_4\{\frac{W^2(t) - W^2(t_0)}{2} - \frac{(t-t_0)}{2} - W(t_0)(W(t) - W(t_0))\}, \\
&= \frac{K_4}{2}\{W^2(t) - W^2(t_0) - 2W(t_0)(W(t) - W(t_0)) - (t-t_0)\}, \\
&= \frac{K_4}{2}\{(W(t) - W(t_0))^2 - (t-t_0)\}, \\
&= \frac{K_4}{2}[\Delta W^2(t_n) - \Delta t], \\
&= \mathscr{O}(\Delta t^1).
\end{aligned} \tag{2.51}$$

This is the local truncation error of the stochastic integral (2.42). To get the global truncation error of the same integral, addition of variances to local truncation errors is needed to get the global variance truncation error instead of summing local errors at each time step. This is due to the fact that Wiener process increments are independent at each time step size Δt. With this fact the global truncation error of stochastic integral is of $\mathscr{O}(\Delta t^{\frac{1}{2}})$, Milstein scheme has $\mathscr{O}(\Delta t)$ and $\mathscr{O}(\Delta t^{\frac{1}{2}})$ order of convergence in strong sense for scalar and vector equations respectively. Euler scheme and Milstein scheme have the same order of convergence in weak sense. The following equation presents Milstein scheme in one dimension:

$$\begin{aligned}
X(t) = X(t_0) + \mu(t_0, X(t_0))\Delta t_0 + \sigma(t_0, X(t_0))\Delta W(t_0) + \frac{1}{2}\sigma(t_0, X(t_0))\frac{\partial \sigma}{\partial x}\{[W(t) - W(t_0)]^2 \\
- (t - t_0)\} + Err_2.
\end{aligned} \tag{2.52}$$

More analysis can be made from the error term of equation (2.47) to get more higher order of convergence of new scheme.

2.4.2 Numerical schemes

In order to have right approximate of the solution, selection of the numerical scheme is very important Kloeden and Platen (2013) and Øksendal (2003). Schemes presented in this work can be used to Stratonovich or *Itô* SDEs.

2.4.3 Euler scheme

The Euler scheme is derived through Taylor expansion of the *Itô* stochastic differential equation. For one dimensional *Itô* SDE, the Euler scheme is:

$$X_{n+1} = X_n + \mu(t_n, X_n)\Delta t_n + \sigma(t_n, X_n)\Delta W(t_n). \tag{2.53}$$

Incase of two dimensional *Itô* SDEs, the Euler scheme is:

$$X_{n+1} = X_n + \mu(t_n, X_n)\Delta t_n + \sigma(t_n, X_n)\Delta W_1(t_n), \tag{2.54}$$

$$Y_{n+1} = Y_n + \mu(t_n, X_n)\Delta t_n + \sigma(t_n, X_n)\Delta W_2(t_n). \tag{2.55}$$

Note that $Y(t) = X_2(t)$. At times $t_n = \sum_{i=0}^{n-1} \Delta t_i$, the scheme provides discrete approximations $X_n \approx X(t_n)$.

2.4.4 Milstein scheme

Equation (2.46) described in section (2.4) represent the Milstein scheme. In scalar SDEs, the Milstein scheme has more accuracy compared to Euler scheme. The Milstein scheme for one dimensional is:

$$X_{n+1} = X_n + \mu(X_n, t_n)\Delta t_n + \sigma(X_n, t_n)\Delta W(t_n) + \frac{1}{2}\sigma(X_n, t_n)\frac{\partial \sigma}{\partial x}(\Delta W^2(t_n) - \Delta t). \tag{2.56}$$

Incase of two dimensional *Itô* SDEs, the Milstein scheme is:

$$X_{n+1} = X_n + \mu(X_n, t_n)\Delta t_n + \sigma(X_n, t_n)\Delta W(t_n) + \frac{1}{2}\sigma(X_n, t_n)\frac{\partial \sigma}{\partial x}(\Delta W^2(t_n) - \Delta t), \tag{2.57}$$

$$Y_{n+1} = Y_n + \mu(Y_n, t_n)\Delta t_n + \sigma(Y_n, t_n)\Delta W(t_n) + \frac{1}{2}\sigma(Y_n, t_n)\frac{\partial \sigma}{\partial y}(\Delta W^2(t_n) - \Delta t). \tag{2.58}$$

The most important thing to consider before the use of Milstein scheme is the existance of partial derivative of the diffusion coefficient.

2.4.5 Heun scheme

The Heun scheme is the predictor-corrector scheme which is applicable to Stratonovich SDE only. Thus, in order to apply Heun scheme for *Itô* SDE, transformation of the *Itô* SDE to Stratonovich is required. This can be done through the use of the relation between *Itô* and Stratonovich discussed in section (2.2). An example of the Heun Scheme is:

$$X^*_{n+1} = X_n + \mu(X_n, t_n)\Delta t_n + \sigma(X_n, t_n)\Delta W(t_n), \tag{2.59}$$

$$X_{n+1} = X_n + \frac{1}{2}\{\mu(X_n, t_n) + \mu(X^*_{n+1}, t_{n+1})\}\Delta t_n + \frac{1}{2}\{\sigma(X_n, t_n) + \sigma(X^*_{n+1}, t_{n+1})\}\Delta W(t_n), \tag{2.60}$$

$$Y^*_{n+1} = Y_n + \mu(Y_n, t_n)\Delta t_n + \sigma(Y_n, t_n)\Delta W(t_n), \tag{2.61}$$

$$Y_{n+1} = Y_n + \frac{1}{2}\{\mu(Y_n, t_n) + \mu(Y^*_{n+1}, t_{n+1})\}\Delta t_n + \frac{1}{2}\{\sigma(Y_n, t_n) + \sigma(Y^*_{n+1}, t_{n+1})\}\Delta W(t_n). \tag{2.62}$$

There is a strong order of convergence $\mathcal{O}(\Delta t^1)$ in the Heun scheme. More discussion on schemes for finding solution of SDEs are found in Kloeden and Platen (2013).

2.4.6 Strong and Weak order of convergence

Accuracy of the method to approximate SDEs can be measured in two ways by considering order of convergence: strong and weak. More discussion on these concepts can be found in Kloeden and Platen (2013) and Higham (2001).

Strong convergence

By strong convergence, the solution provided by the scheme selected (chosen) must match to the exact solution more closely as possible Higham (2001).

Definition [1] Strong order of convergence

A method can have a strong order of convergence α_1, if there existance of a positive constant K such that:

$$E\{|X_T - X_n|\} \leq K(\Delta t)^{\alpha_1}. \tag{2.63}$$

For any fixed $T = n\Delta t \varepsilon [0,T]$ and Δt is sufficiently small positive constant. Example. Consider the following vector *Itô* SDE, with zero initial condition.

$$dX_t = dW_t, \tag{2.64}$$

$$dY_t = X_t dW_t, \tag{2.65}$$

$$X_t = W_t,$$

$$dY_t = W_t dW_t.$$

The exact solution of this equation will be:

$$Y_T = \int_0^T W_s dW_s = \frac{W^2(T)}{2} - \frac{T}{2}.$$

By using the Euler scheme to approximate solution:

$$X_n = X_{n-1} + \Delta W_{n-1} = \sum \Delta W_i = W_n,$$
$$Y_n = X_{n-1}\Delta W_{n-1} = W_{n-1}\Delta W_{n-1} = \sum W_{i-1}(W_i - W_{i-1}),$$

Thus:

$$E\{(Y_T - Y_n)^2\} = E\{(\frac{W^2(T)}{2} - \frac{T}{2}) - \sum W_{i-1}(W_i - W_{i-1})^2\}.$$

The variance has the error=$\mathcal{O}(\Delta t)$and thus the scheme has strong convergence of order $\mathcal{O}(\Delta t^{\frac{1}{2}})$

Weak convergence

The strong convergence always measures the rate of mean error decay. Alternatively to this approach is to measure the rate of decaying of the "error of mean" and hence this lead to the concept of weak convergence.

Definition[2] Weak order of convergence

A method can have weak order of convergence α_2, if there exist a positive constant K, such that

$$|E\{h(X_T,T)\} - E\{h(X_n,n)\}| \leq K(\Delta t)^{\alpha_2}. \tag{2.66}$$

For any fixed $T = n\Delta t \varepsilon [0,T]$,Δt is sufficiently small positive constant and h is the function with polynomial growth.

The following figure shows the relationship between the Exact solution and Euler approximate solution to a well known Black-Scholes partial differential equation whose exact solution is;

$$X(t) = X(0)exp((\lambda - \frac{1}{2}\mu^2)t + \mu W(t)).$$

The exact solution is plotted with the following values, $\lambda = 2, \mu = 1$, and $X_0 = 1$ and discretization of Brownian path over $[0,1]$ with $\delta t = 2^{-8}$. The Euler method were applied by considering the stepsize $\Delta t = R\delta t$, with $R = 4$. The code for Fig. 3 was written by Higham (2001).

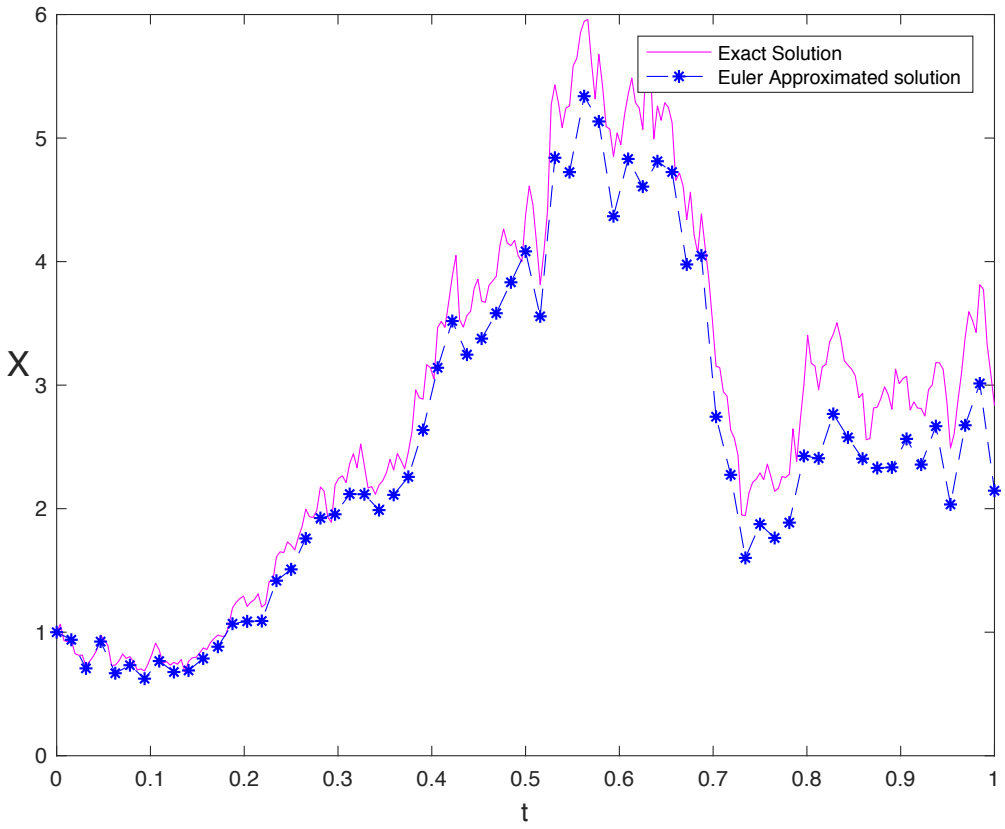

Figure 3: Exact solution and Euler approximation.

From the figure above one can notice that, the Euler approximate solution becomes more closely to exact solution as Δt is decreasing. This means convergence is taking place.

CHAPTER THREE

MATERIALS AND METHODS

This chapter describes various methods, materials, and techniques that have been employed to develop stochastic model for sediment transport. It also presents other concepts that are of paramount important in developing model.

3.1 Model development

The particle model developed in this section for sediment transport in ports and harbours, was developed by showing consistency between the Eulerian model for sediment transport and the Kolmogorov Foward equation. The Eulerian model for sediment transport includes erosion term as a constant and deposition term as a variable.

3.2 Shallow water flow equations

In describing sediment transport problems in ports and harbors, the particle model requires input such as water depth $H(x,y,t)$, water level ξ, velocities of flowing water $[U(x,y,t),V(x,y,t)]^T$ and so forth, with the assumption that these inputs satisfy shallow water flow equations. The mass and momentum exchange of sediment mixture are given by the following shallow water equations (3.1-3.3) Mahera and Narsis (2013).

$$\frac{\partial U}{\partial t}+U\frac{\partial U}{\partial x}+V\frac{\partial U}{\partial y}+g\frac{\partial \xi}{\partial x}-fV+g\frac{U(U^2+V^2)^{\frac{1}{2}}}{(C_Z)^2H}=0, \tag{3.1}$$

$$\frac{\partial V}{\partial t}+U\frac{\partial V}{\partial x}+V\frac{\partial V}{\partial y}+g\frac{\partial \xi}{\partial y}-fU+g\frac{V(U^2+V^2)^{\frac{1}{2}}}{(C_Z)^2H}=0. \tag{3.2}$$

Since the vertical velocity is considered to be uniform, the fall and rise of the free surface are given by the following continuity equation:

$$\frac{\partial H}{\partial t}+\frac{\partial (UH)}{\partial x}+\frac{\partial (VH)}{\partial y}=0,. \tag{3.3}$$

where, t, x and y are time and cartesian coordinate in two dimensional, U and V are the velocity in horizontal and vertical directions respectively, $H=h+\xi$ represents the total depth where h represents depth of the water and ξ stands for water, C_z is the bottom friction coefficient known as the Chezy coefficient, g represents acceleration due to gravity and f is the Coriolis parameter.

3.3 Eulerian model for sediment transport

The Eulerian transport model is used to describe the dynamics of suspended particles. It is modified by considering non-cohesive type of sediment particles. This is similar to that in Mahera and Narsis (2013), however, with modification on the deposition parameter β. In Mahera and Narsis (2013), β is considered to be a constant with the value approximated to $4 \times 10^{-3} s^{-1}$ for fine sand but in this model, β is considered to be a function that relates β to settling velocity ω_s and a diffusion coefficient (K) as done in Van Rijn *et al.* (1990). The Eulerian model is as shown below:

$$\frac{\partial(HVC)}{\partial y} + \frac{\partial(HC)}{\partial t} + \frac{\partial(HUC)}{\partial x} - \left(\frac{\partial}{\partial x}(K\frac{\partial HC}{\partial x}) + \frac{\partial}{\partial y}(K\frac{\partial HC}{\partial y}) \right) = -\beta HC + \varepsilon(U,V).\eta_s, \tag{3.4}$$

where: β is the deposition coefficient, $\varepsilon(U,V) = (U^2 + V^2)(m^2 s^{-1})$ stands for flow velocities function, η_s is the erosion coefficient, $\varepsilon(U,V).\eta_s$ models sediment particles erosion. The term βHC models sediment deposition. $\eta_s = 0.0001(kgm^{-4}s)$ as reported by Schuttelaars and De Swart (1997) and β is given by equation (3.5) below:

$$\beta = \frac{\omega_s^2}{K}, \tag{3.5}$$

where: ω_s represents settling velocity of naturally sediment which is given by equation (3.6) below

$$\omega_s = \sqrt{(13.95\frac{\nu}{d})^2 + 1.09(\frac{\rho_s}{\rho_w} - 1)gd} - 13.95\frac{\nu}{d}, \tag{3.6}$$

The settling velocity is estimated in m/s, ν represents water viscosity, d is the sediment diameter, ρ_s represent sediment densities, ρ_w represents water densities and g represents the acceleration due to gravity. The diameter of the sediment for the dimensionless particle:

$$d_* = d_{50}\left[(\frac{\rho_s}{\rho_w} - 1)\frac{g}{\upsilon^2} \right]^{\frac{1}{3}}. \tag{3.7}$$

where: d_{50} represents the median of diameters. The diffusion coefficient K in equation (3.5) is taken as $0.01 m^2 s^{-1}$ following the study of Garrabou and Flos (1995) who performed tracer experiments to estimate diffusion values.

3.3.1 Bed level changes by using Eulerian transport model

Equation (3.8) below is used to determine the bed-level changes in every grid cell:

$$\frac{\partial h}{\partial t} = (\beta_e - \eta_e)\frac{1}{(1-\Psi)\rho_s}, \tag{3.8}$$

where: Ψ represents the sea bed porosity, $\beta_e = \varepsilon(U,V).\eta_s$ and $\eta_e = \beta HC$ represents the erosion term and the deposition term, respectively. With the assumption that erosion and deposition terms balances, the simplified model was developed from Equation (3.4). The model developed found to be consistent with the Langragian particle model.

$$\beta HC = (U^2 + V^2).\eta_s, \tag{3.9}$$

sediment transport in water along horizontal and vertical directions is presented by $Q_x = UCH$ and $Q_y = VCH$ respectively in which U and V stands for velocity components in horizontal and vertical directions respectively, C represents concentration of sediment particles and H stands for water depth in a grid cell. Writing Q_x and Q_y in vector form that is $\bar{Q} = [Q_x, Q_y]^T$ and with the use of Equation (3.9) the following Equation is obtained.

$$\bar{Q} = [U.(U^2 + V^2).f_d, V.(U^2 + V^2).f_d]^T, \tag{3.10}$$

where: $f_d = \frac{\eta_s}{\beta}$ represents the drag force. To account for the amount of mass entering or exit a given location, the divergence is considered. The divergence gives the rate of mass added in the grid cell.

$$\frac{\partial m}{\partial t} = -div(\bar{Q}), \tag{3.11}$$

where: div stands for divergence and $\bar{Q} = \frac{1}{T}\int_0^T Q dt$. Therefore, the Equation (3.11) describes how much mass exits or enters the cell under the assumption that there is no creation or destruction of matter within the cell. To examine the effect of sediment particles transportion on sea bedforms, equation (3.12) can be used to examine change in bedlevel:

$$\frac{\partial h}{\partial t} = \frac{\partial m}{\partial t}\frac{1}{\rho_s(1-\Psi)}. \tag{3.12}$$

Applying schemes of finite difference the bedlevel change is estimated by using the equation (3.13).

$$\frac{\partial h}{\partial t} = \frac{1}{(1-\Psi)\rho_s}.div(\bar{Q}). \tag{3.13}$$

When $v = 0$, the following equation is used to describe the transport:

$$\frac{\partial h}{\partial t} = -\frac{f_d}{(1-\Psi)\rho_s}.div(\bar{U}^3). \tag{3.14}$$

Thus, by using Equations (3.11) and (3.12), the following Equation is used to determine the bed level change:

$$\triangle h \approx \frac{-f_d T}{(1-\Psi)\rho_s}.(\frac{\partial U_m}{\partial x} + \frac{\partial V_m}{\partial y}), \tag{3.15}$$

where:

$$U_m = \frac{1}{T}\int_0^T (U^2+V^2)U dt, \tag{3.16}$$

$$V_m = \frac{1}{T}\int_0^T (U^2+V^2)V dt. \tag{3.17}$$

3.4 A model for transporting sediment particle in ports and harbours

A sediment particle model is used to describe and predict effectivelly sediment transport with the use of random walk models Man and Tsai (2007) and Oh and Tsai (2010). A Random Walk model is a stochastic differential equation which can be used to describe a path-valued process: It has the following two parts namely deterministic and stochastic.

3.4.1 Integrating movement of sediment particles

The following is 2-dimwnsional SDEs developed in this section.

$$dX(t) \overset{it\hat{o}}{=} \left[U + \frac{K}{H}(\frac{\partial H}{\partial x}) + \frac{\partial K}{\partial x}\right] dt + \sqrt{2K} dB_1(t), \tag{3.18}$$

$$dY(t) \overset{it\hat{o}}{=} \left[V + \frac{K}{H}(\frac{\partial H}{\partial y}) + \frac{\partial K}{\partial y}\right] dt + \sqrt{2K} dB_2(t), \tag{3.19}$$

where: $B_1(t)$ and $B_2(t)$ are Gaussian Brownian processes, and $K(x,y,t)$ stands for dispersion coefficient of sediment particles. $V(x,y)$ and $U(x,y)$ represents flow velocities in vertical and horizontal directions respectively, $H(x,y)$ represent water depth, $dB_1(t)$ and $dB_2(t)$ represents independent increment of Brownian motion.

3.4.2 Sediment particles in deposition state

In this section, the binary state is used for describing the state of sediment particle at any specified time t.

$$S(X,Y)_t = \begin{cases} 1 \text{ suspension state} \\ 0 \text{ deposition state} \end{cases}$$

For the particle in suspension state, the interest is on the transition from state 1 to state 0. The following equation (3.20) can be used to model this transition in continuous form:

$$\frac{dPr(S(X,Y)_t = 1)}{dt} = -\beta . Pr(S(X,Y)_t = 1), \text{initially} Pr(S(X,Y)_0 = 1) = 1, \tag{3.20}$$

where: β represent deposition coefficient given by equation (3.5) and $Pr(S(X,Y)_t = 1)$ defines the probability state of the particle at time $t = 1$. Evolution of the particle in flow is given by the transition probability equation (3.21) below.

$$Pr(S(X,Y)_{(t+\triangle t)}) = 1 \mid S(X,Y)_t = 1) = Pr(S(X,Y)_0 = 1).[1-\beta.\triangle t]. \tag{3.21}$$

With the assumption that the turbulence patterns and flow fields are constant with the time step period, then the probability that sedimentation of a particle will occur is given by the equation (3.22) below:

$$Pr(S(X,Y)_{t+\triangle t}) = 0 \mid S(X,Y)_t = 1) = \beta.\triangle t. \tag{3.22}$$

3.4.3 Sediment particles in suspension state

Group of particles concentration at a particular location are always represented by mass. With the inclusion of the source term in the model, the expected number of partticles in suspension state at a given time t for every grid cell, will be given by Equation (3.23) through drawing a number out of a defined Poisson distribution function.

$$\text{Expected number of particles} = \frac{\triangle x.\eta_s.\triangle t.\triangle y.(U^2+V^2)}{M_p}, \tag{3.23}$$

where: $\triangle x =$ stands for grid cell width in x-direction, $\triangle y =$ stands for grid cell width in y-direction, $\triangle t =$ stands for time step size, $\eta_s =$ stands for erosion coefficient, $M_p =$ Is the mass of each particle.

3.5 The Relationship between Eulerian transport model and the Fokker-Planck equation

The most important assumption in showing the relationship between the particle model (3.18 -3.19) and the Eulerian transport model is that the mass expectation of a particle at position (x,y) at a time t is given by equation (3.24) which is called a mass density of a particle defined in a unit area.

$$\prec m(x,y,t) \succ = Pr(S(X,Y)_t = 1).f(x,y,t). \tag{3.24}$$

In deriving the Fokker-Planck equation that includes sedimentation and particles in suspension state, Let K stand for diffusion coefficient as discussed in section (3.3), $\prec m(x,y,t) \succ$ for mass density of a particle per unit area, $f(x,y,t)$ for probability density function of the particle position and $Pr(S(X,Y)_t = 1)$ for probability of the particle in suspension state. By using SDEs (3.8

-3.9) the probability $f(x,y,t)$ results due to the well known Fokker Planck equation Heemink (1990).

$$\frac{\partial f(x,y,t)}{\partial t} = -\frac{\partial}{\partial x}\left[(U+\frac{K}{H}\frac{\partial H}{\partial x}+\frac{\partial K}{\partial x}).f(x,y,t)\right] - \frac{\partial}{\partial y}\left[(V+\frac{K}{H}\frac{\partial H}{\partial y}+\frac{\partial K}{\partial y}).f(x,y,t)\right] + \frac{1}{2}\frac{\partial^2}{\partial x^2}(f(x,y,t).2K) + \frac{1}{2}\frac{\partial^2}{\partial y^2}(f(x,y,t).2K). \quad (3.25)$$

In this section, the model (3.8-3.9) is extended by including erosion and deposition terms. Starting with differentiating equation (3.24) with respect to time t, the Fokker-Planck equation can be derived as follows:

$$\frac{\partial}{\partial t} \prec m(x,y,t) \succ = \frac{\partial}{\partial t} f(x,y,t) Pr(S(X,Y)_t = 1) + \frac{\partial}{\partial t} Pr(S(X,Y)_t = 1) f(x,y,t). \quad (3.26)$$

By using equation (3.22) in (3.26) equation (3.27) is obtained.

$$\frac{\partial}{\partial t} \prec m(x,y,t) \succ = Pr(S(X,Y)_t = 1)\frac{\partial}{\partial t} f(x,y,t) - \beta f(x,y,t) Pr(S(X,Y)_t = 1). \quad (3.27)$$

By adding the erosion term to equation (3.27) the following equation (3.28) is obtained:

$$\frac{\partial}{\partial t} \prec m(x,y,t) \succ = Pr(S(X,Y)_t = 1)\frac{\partial}{\partial t} f(x,y,t) - \beta f(x,y,t) Pr(S(X,Y)_t = 1) + \varepsilon(U,V).\eta_s. \quad (3.28)$$

By multiplying $Pr(S(X,Y)_t = 1)$ on both sides of equation (3.25) to get (3.29):

$$\frac{\partial f(x,y,t)}{\partial t}.Pr(S(X,Y)_t = 1) = -\frac{\partial}{\partial x}\left[(U+\frac{K}{H}\frac{\partial H}{\partial x}+\frac{\partial K}{\partial x}).f(x,y,t).Pr(S(X,Y)_t = 1)\right] - \frac{\partial}{\partial y}\left[(V+\frac{K}{H}\frac{\partial H}{\partial y}+\frac{\partial K}{\partial y}).f(x,y,t).Pr(S(X,Y)_t = 1)\right] + \frac{1}{2}\frac{\partial^2}{\partial x^2}(f(x,y,t).2K.Pr(S(X,Y)_t = 1) + \frac{1}{2}\frac{\partial^2}{\partial y^2}(f(x,y,t).2K.Pr(S(X,Y)_t = 1)). \quad (3.29)$$

Using equation (3.29) in (3.28), the following Fokker-Planck equation (3.30) with erosion and deposition term is obtained:

$$\frac{\partial}{\partial t} \prec m(x,y,t) \succ = -\frac{\partial}{\partial x}\left[(U+\frac{K}{H}\frac{\partial H}{\partial x}+\frac{\partial K}{\partial x}). \prec m(x,y,t) \succ\right] - \frac{\partial}{\partial y}\left[(V+\frac{K}{H}\frac{\partial H}{\partial y}+\frac{\partial K}{\partial y}). \prec m(x,y,t) \succ\right] + \frac{1}{2}\frac{\partial^2}{\partial x^2}(\prec m(x,y,t) \succ .2K) + \frac{1}{2}\frac{\partial^2}{\partial y^2}(\prec m(x,y,t) \succ .2K) - \beta \prec m(x,y,t) \succ + \varepsilon(U,V).\eta_s. \quad (3.30)$$

The concentration of particles represented by $C(x,y,t)$ given in kg/m^3 is related to this particles' mass located at (x,y) through equation (3.31) given below:

$$C(x,y,t) = \frac{\prec m(x,y,t) \succ}{H(x,y,t)}. \tag{3.31}$$

By substituting equation (3.31) into the Fokker-Planck equation (3.30) the Eulerian sediment transport equation (3.4) can be derived, as in equation (3.32).

$$\frac{\partial(HC)}{\partial t} + \frac{\partial(HUC)}{\partial x} + \frac{\partial(HVC)}{\partial y} - \frac{\partial}{\partial x}(D\frac{\partial HC}{\partial x}) - \frac{\partial}{\partial y}(D\frac{\partial HC}{\partial y}) = -\beta HC + \varepsilon(U,V).\eta_s. \tag{3.32}$$

Thus, it is shown that the model (3.18-3.23) is consistent with the model (3.4). This means that, one can either solve equation (3.4) numerically or simulate the stochastic equation (3.18 -3.19) for different many particles.

3.6 Numerical approximation of the particle model

3.6.1 Boundaries

In most cases, the numerical integration of particle position becomes a problem because of boundary conditions. In finding a new location from the given location, one may find the new location is outside the boundary which may cause the phenomenon to be physically impossible. In this work the following boundary conditions are considered: open boundary conditions and closed boundary conditions. Closed boundaries relate to the domains such as banks, coast lines, and sea beds. Open boundaries depend on modeler's decisions to limit outside regions (artificially) which are of no interest or because at these locations there is no domain information. It is natural for particles to cross the open boundary and in this work such case is not within the scope of the model. When particles cross closed boundary for both the drift step and diffusive step of integration respectively, the rules 1 and 2 below apply:

(i) Reduce the integration time to $2^{-n}\triangle t$ by halving the time step taken n-times, this makes the remaining integration time to be $(1-2^{-n})\triangle t$. Thus, to make the full time step $\triangle t$ complete, at least $2^n - 1$ steps are needed. Note that this reduction process, affects only the current time step and the remaining sub steps remains unaffected. This approach is very useful in modelling shear stress along the coastline.

(ii) Maintain step 1 above and restore the state of white noise process in advance to invalidated the steps of integration. Repeat the halving process until integration of the full time $\triangle t$ time step is done without crossing the boundary.

3.6.2 Flux of sediment particles at open boundaries

To encounter the difference of sediment particles entering into and departing outside the domain, particle flux concept can be used. As it is natural for particles to flow outside the domain, there is no need of controlling particles flowing out. Once the particle crosses an open boundary integration process stops as there is no domain information which is given. By considering the above mentioned reasons, model for the particles flowing in is developed as shown below:

$$\text{Expected number of particles} = \begin{cases} \dfrac{\triangle y.\eta_s.\triangle t.V.(U^2+V^2)}{\beta M_p} \text{ flow of sediment particles parallel to y-axis} \\ \dfrac{\triangle x.\eta_s.\triangle t.U.(U^2+V^2)}{\beta M_p} \text{flow of sediment particles parallel to x-axis} \end{cases} \tag{3.33}$$

In each iteration, the above developed expectation value is used to find the possible number of sediment particles increased in the domain boundary with the use of Poisson distribution.

3.7 Changes in bed level by using particle model

Since a particle model for sediment transport is developed, there is a need of developing equations that will be applied to examine the change in bed level using the model developed. This can be done as follows; Consider the simplified form of equation (3.4) by assuming change in mass locally, $\dfrac{\partial m}{\partial t} \approx \beta_e - \eta_e$ and assumptions made in section (3.3.1). The equation (3.34) below, can be used to find the approximate mass value for every grid cell with respect to time.

$$\frac{\partial m}{\partial t} = \frac{\triangle N_p}{\triangle t}\frac{1}{\triangle x \triangle y} M_p. \tag{3.34}$$

By using the approximate $\dfrac{\partial m}{\partial t} \approx \beta_e - \eta_e$ and equation (3.8) the change in bed level equation is derived as follows, equation (3.35):

$$\frac{\partial h}{\partial t} = \frac{\triangle N_p}{\triangle t}\frac{1}{\rho_s(1-\Psi)\triangle x \triangle y} M_p. \tag{3.35}$$

where: M_p stands for mass of each particle, ρ_s stands for density of a particle, Ψ stands for the bed porosity, $\triangle N_p$ stands for the difference in number of particles in deposition and suspension state for each grid cell i,j. Thus, the following equations are used to determine the accumulated change in bed level:

$$\triangle h = \int_0^T \frac{\partial h}{\partial t} dt, \tag{3.36}$$

$$\triangle h \approx \Sigma \frac{\triangle N_p}{\rho_s (1-\Psi) \triangle x \triangle y} M_p. \tag{3.37}$$

CHAPTER FOUR

RESULTS AND DISCUSSION

4.1 Introduction

In this chapter, numerical simulations of the particle model developed in Section (3.4) is provided by considering three test environment.In each test environment I, II and III three functions D, H, and U, V were considered and two of them were taken as constant while some profile is taken for the other function. In each case discussion on simulation obtained is provided.

4.2 Simulation of the particle model

This section contains simple experiments to simulate the particle model developed in section (3) to show the distribution of particles in suspension and deposition using MATLAB. As many SDEs have no analytic solution, there are so many ways (schemes) which can be applied to solve SDEs systems so as to get numerical solution. These schemes includes: Euler scheme, Milstein scheme and Heun Scheme. In this work the Euler scheme which has $\frac{1}{2}$ and 1 order of convergence in strong and weak sense respectively, was used to approximate the solution of the *Itô* SDEs. The discretization process of the two dimensional SDEs was done in a similar approach as in Heemink (1990). The following is the approximate solution of the SDEs by using Euler scheme for $t_0 < t_1 < t_2 ... < t_N = T$ of $[t_0, T]$.

$$\bar{X}(t_{n+1}) = \bar{X}(t_n) + \left[U + (\frac{K}{H}\frac{\partial H}{\partial x}) + \frac{\partial K}{\partial y} \right] \triangle t_n + \sqrt{2K} \triangle B_1(t_k), \tag{4.1}$$

$$\bar{Y}(t_{n+1}) = \bar{Y}(t_n) + \left[V + (\frac{K}{H}\frac{\partial H}{\partial y}) + \frac{\partial K}{\partial y} \right] \triangle t_n + \sqrt{2K} \triangle B_2(t_k), \tag{4.2}$$

$$Pr_{k+1}(S(X,Y)_t = 1) = (1 - \beta(x,y,t)\triangle_k) Pr_k(S(X,Y)_t = 1), \tag{4.3}$$

where: Approximation of $X(t)$ and $Y(t)$ are provided by $\bar{X}(t_{n+1})$ and $\bar{Y}(t_{n+1})$ respectively and $\bar{X}(t_0) = X(t_0) = x_0$ and $y_0 = Y(t_0 = \bar{Y}(t_0))$ are the initial iterations of particles. A domain of 20 by 20 was used to simulate the model $x\varepsilon[-10,10]$ and $y\varepsilon[-10,10]$. The simulation started by releasing 10 000 particles at the centre $(x,y) = (0,0)$. The time step used for all simulations of the model was 0.01 unless otherwise stated, values of the other variables used in the model are found in Table 2. The boundary conditions were treated as described in section (3.6.1). To make

effective simulation of the model the following three test environment which are similar to test environment suggested by Heemink (1990) were considered.Various snapshots for particles positions in suspension and deposition for each test environment were taken at different times as shown in the following figures. Parameters used in Table 2 are found in Zhao *et al.* (2019)

4.2.1 Test Environment I. $U = 3, V = 2.5, H = 10$ and D is a 2D Gaussian Curve

In this test, the water velocities and water depths are set to be constants and the dispersion coefficient D which varies with space. The specific equation for dispersion coefficient is as shown below:

$$D(x,y) = 10 + 10\exp(-0.03(x^2 + y^2)). \tag{4.4}$$

Figure 4 below is the plot of equation (4.4) which shows that after a long time of simulation, particles in suspension and deposition will be uniformly distributed over the domain. The case is verified by Fig. 8 which is a simulations of the particle model with deposition and erosion term at large time t=10.

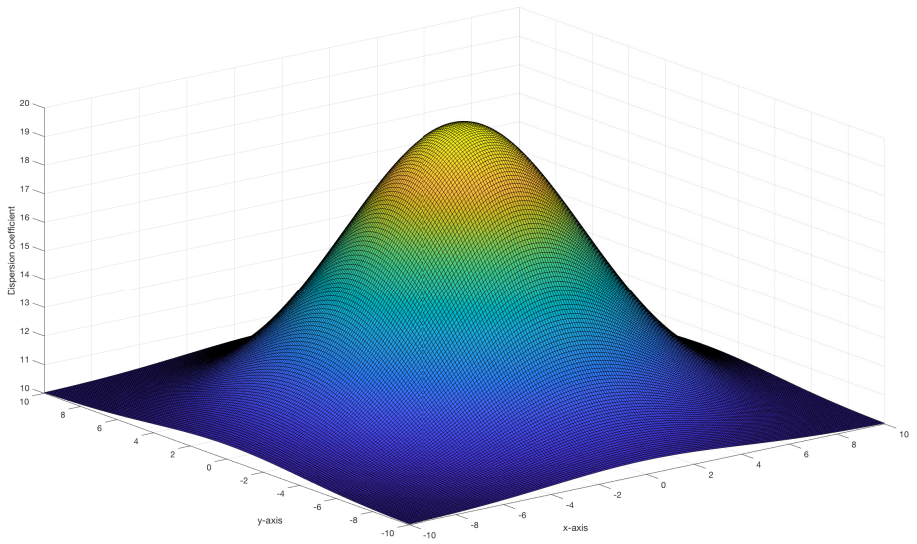

Figure 4: The Gaussian plot for dispersion coeffiecient.

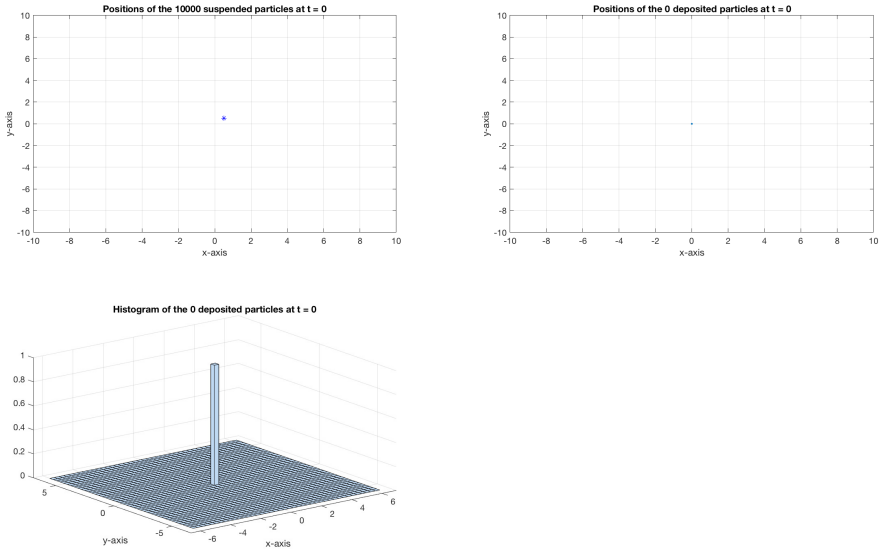

Figure 5: Simulation of the particle model at t=0.

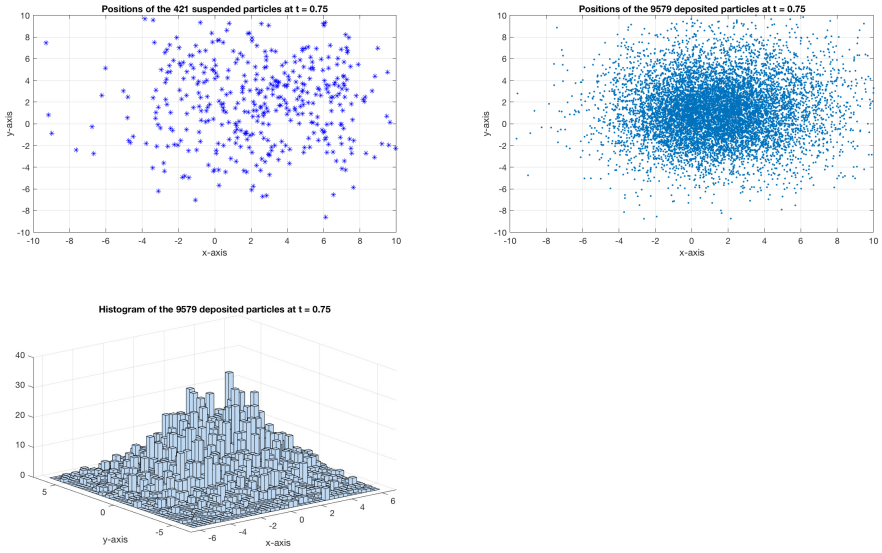

Figure 6: Simulation of the particle model at t=0.5

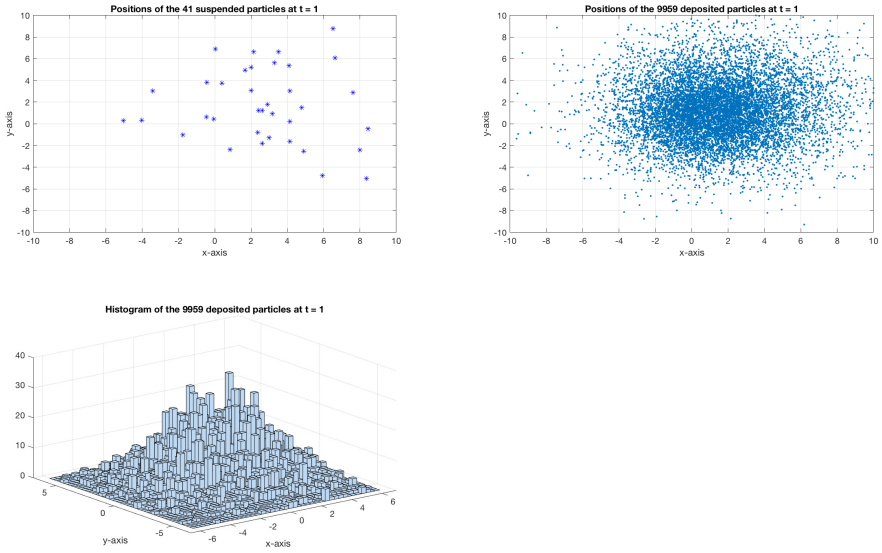

Figure 7: Simulation of the particle model at t=1

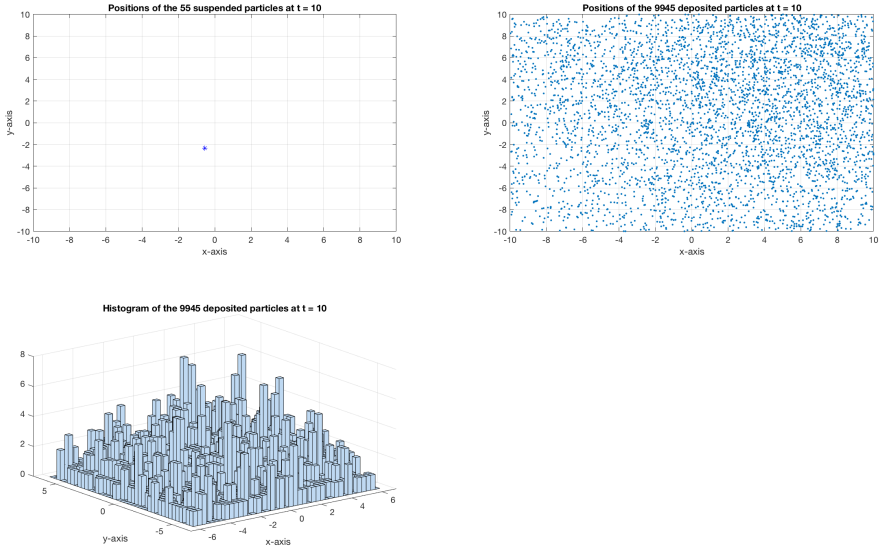

Figure 8: Simulation of the particle model for a large value of time at t=10

In Fig. 5 the simulation was started with the depoyment of 10 000 particle at the middle of the domain $(x,y) = (0,0)$ and during this time(t=0) all 10 000 particles were assumed to be in suspension. Due to change in time the particles are distributed and some are deposited into different locations in the domain due to probabilistic condition developed in section (3). Each simulation indicates the number of particles deposited and remained in suspension for each

iteration but also it shows the histogram of deposited particles to make the event more clear. To confirm that the simulation will give uniform distribution of particles in the domain for a large value of t, simulation of the particle model when t=10 was done and Fig. 8 was obtained, in this simulation the initial time was $t = 0$ and the final time was $t = 10$ and the time steps used was 10. Thus, Fig. 8 proves that the particle distribution is uniformly distributed when simulation is done for a large value of t as it was expected from Fig. 4.

4.2.2 Test Environment II. $U = 3, V = 2.5, D = 10$ and H is a space varying depth

In this test environment water flow velocities and dispersion coefficients are set to be constant while H is the space varying depth. The equation(4.5) below is the specific for depth.

$$H(x,y) = 10 - 5\tanh(x-4) + 5\tanh(x+4). \tag{4.5}$$

Figure (9) is the plot of equation (4.5) which shows that after a long time of simulation, particles distribution is linearly dependent with depth. Thus many particles will be more concentrated at the centre of the domain compared to other parts of the domain. This case is verified by Figs. (10-13) which are simulations of the particle model with deposition and erosion term over various times.

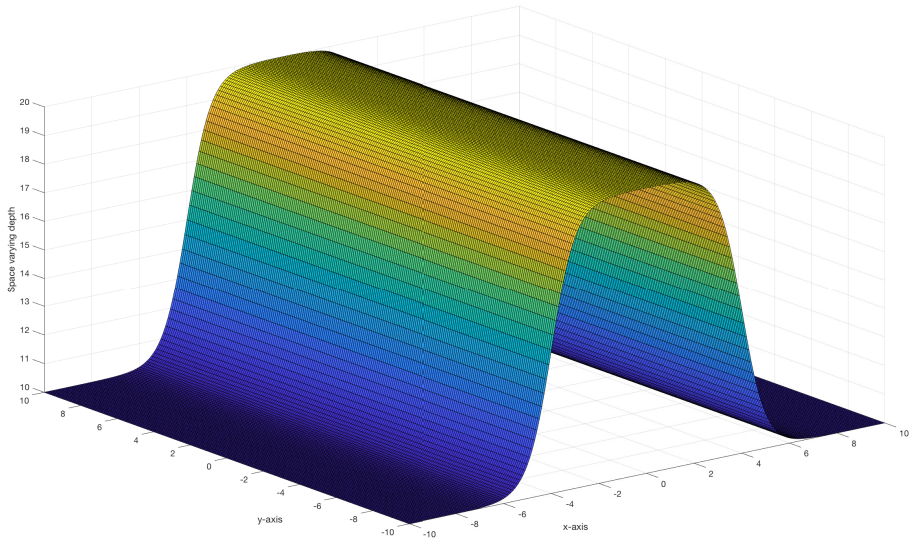

Figure 9: The plot of space varying depth function.

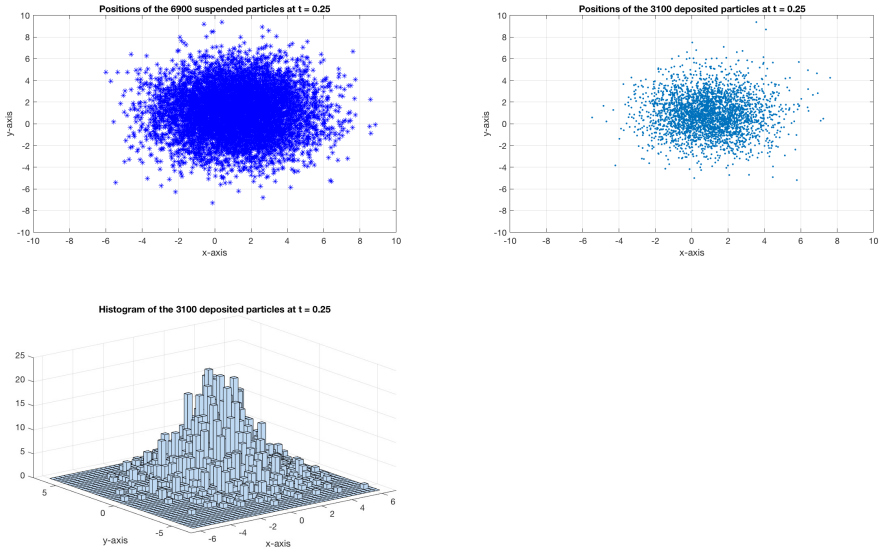

Figure 10: Simulation of the particle model at t=0.25.

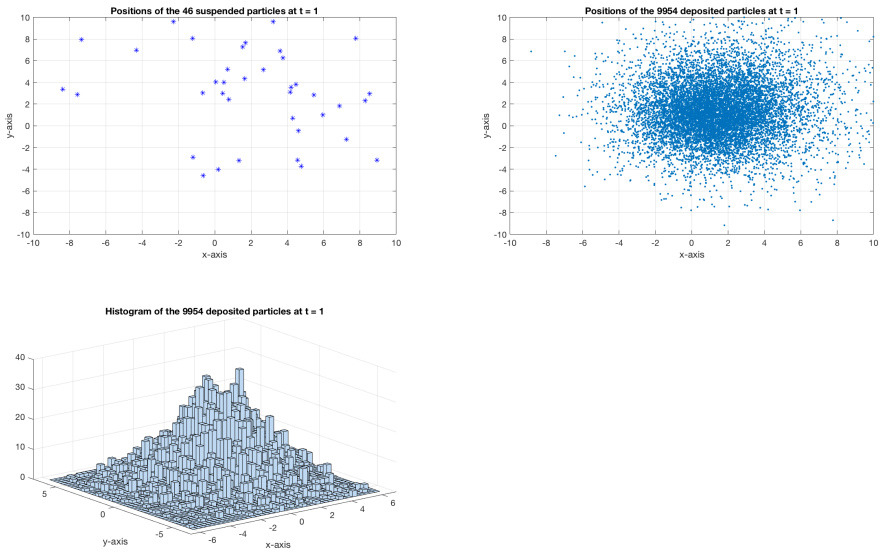

Figure 11: Simulation of the particle model at t=1.

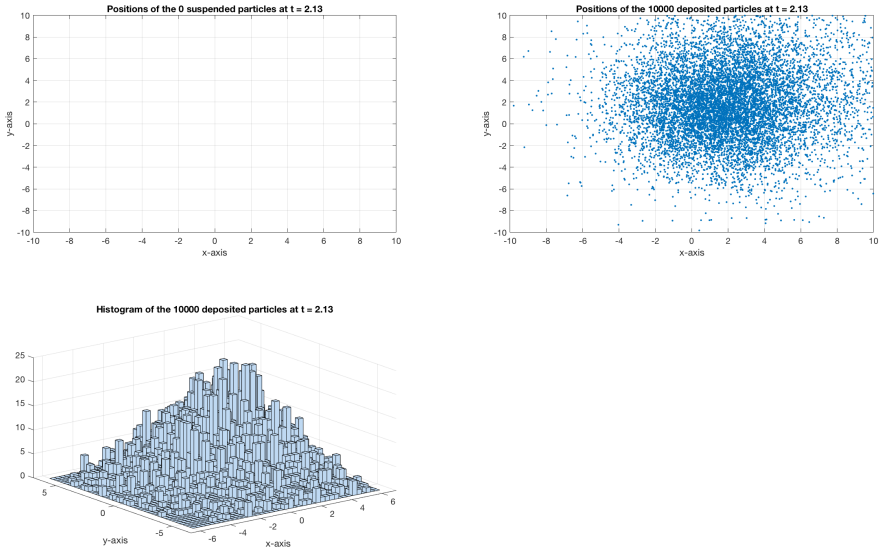

Figure 12: Simulation of the particle model at t=2.13.

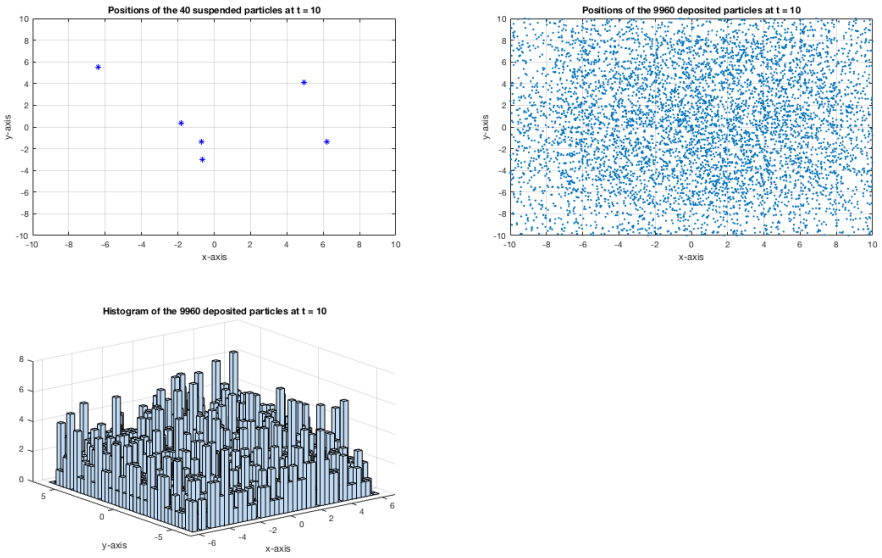

Figure 13: Simulation of the particle model at t=2.13.

Similarly as in environment test I, the simulation was started at t=0 with deployment of 10 000, as time goes on particles are distributed to different parts of the domain. As it is observed from results obtained through Figs. (10-13) particles are distributed in various parts of the domain but many particle are concentrated to the centre of the domain due to deper depth. Thus it is concluded that the large the depth the more the particles will be deposited which is the expected

result from Fig. 9.

4.2.3 Test Environment III $D = 10$ and $H = 10$ U and V are velocities of water flow

In this test the constant depth and contant Dispersion coefficient were considered hence water flow velocities are given by the following specific functions equation (4.6-4.7).

$$U(x,y) = \cos(\frac{\pi x}{20})\sin(\frac{\pi y}{20}). \tag{4.6}$$

$$V(x,y) = -\sin(\frac{\pi x}{20})\cos(\frac{\pi y}{20}). \tag{4.7}$$

In this last test environment, water flow is assumed to be in clockwise rotation so that velocities perpendicular to boundaries are zero, otherwise accumulation of particles will be near the boundary compared to other parts of the domain. Figure (14) shows the vectorfields of water flow velocites in x and y directions.

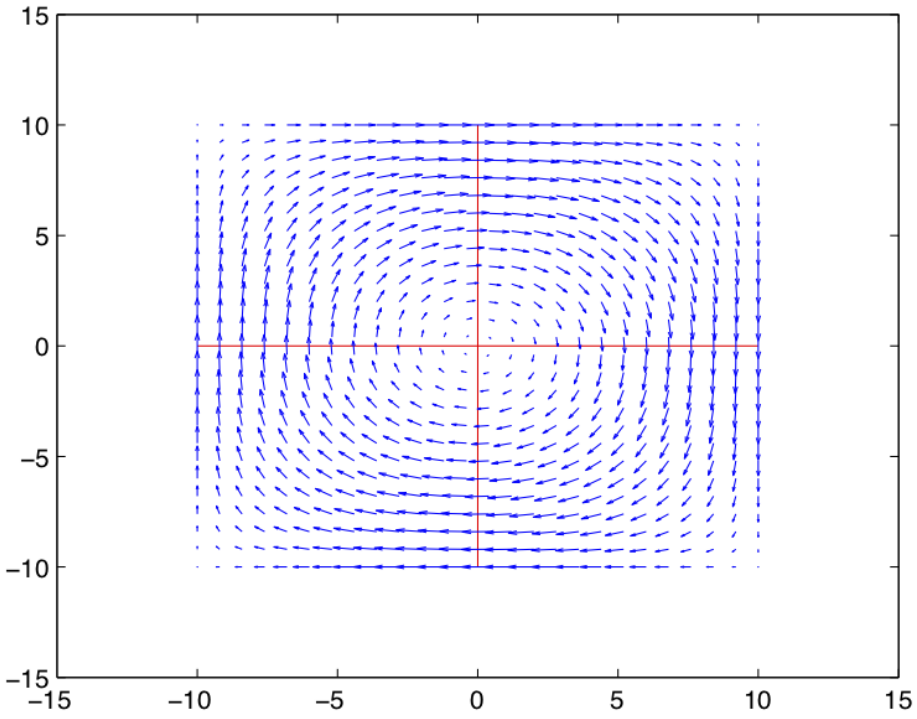

Figure 14: Vector fields of water flow velocities in horizontal and vertical directions.

For a large time simulation, particles in this test environment are expected to be uniformly distributed over the domain, this case is verified by Fig. (15) and Fig. (16).

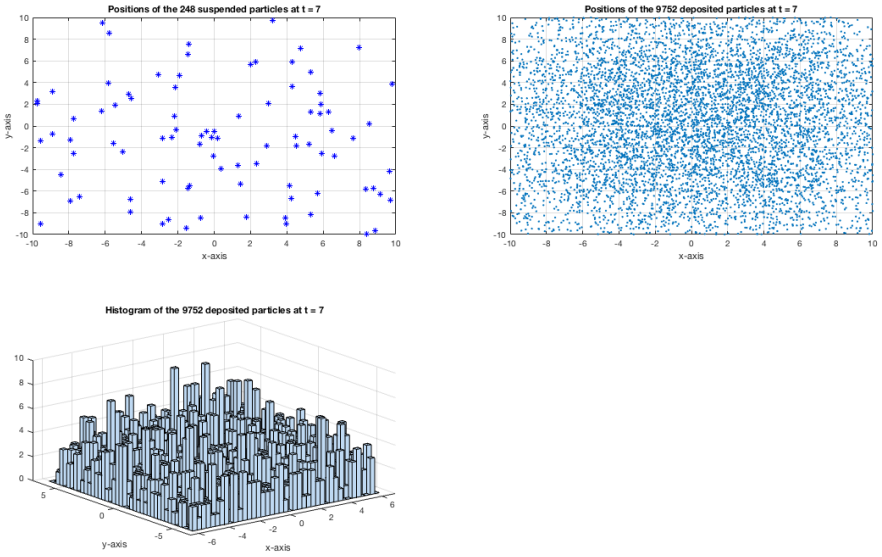

Figure 15: Simulation of the particle model at t=7

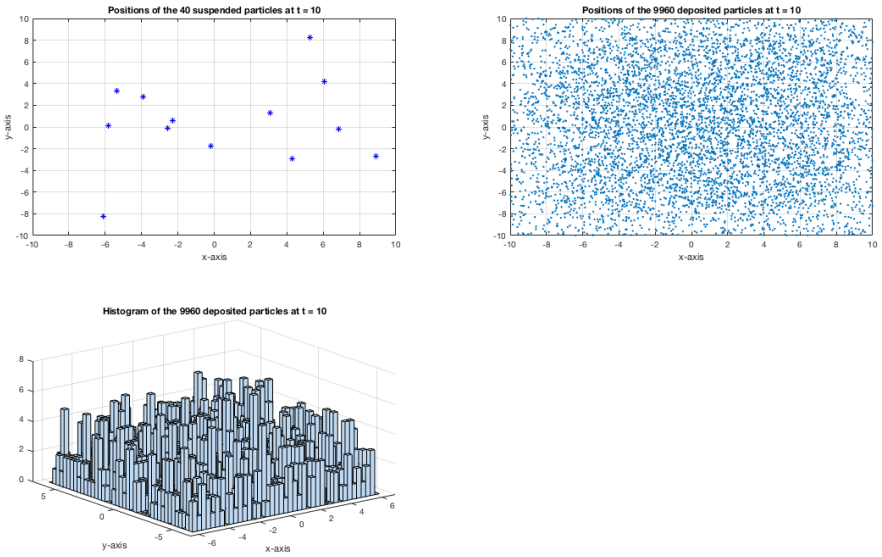

Figure 16: Simulation of the particle model at t=10

To confirm that the simulation will give uniform distribution of particles in the domain for a large value of t as expected, simulation of the particle model when $t = 7$ and $t = 10$ was done and Fig. (15) and Fig. (16) were obtained, in this simulation the initial time was $t = 0$ and the final time was $t = 10$ and the time steps used was 10. Thus as expected Figs. (15-16) proves that particles are uniformly distributed when simulation is done for a large value of t.

4.3 Comparison of the model developed with the stochastic model without erosion and deposition terms

This section carries comparison between the model developed with the selected stochastic model without erosion and depostion to show the differences in particle distribution among the two cases. The selected model among others is the model developed by Heemink (1990). Three environment cases similar to section (4.2) were used to make such comparison and the following snapshots were obtained.

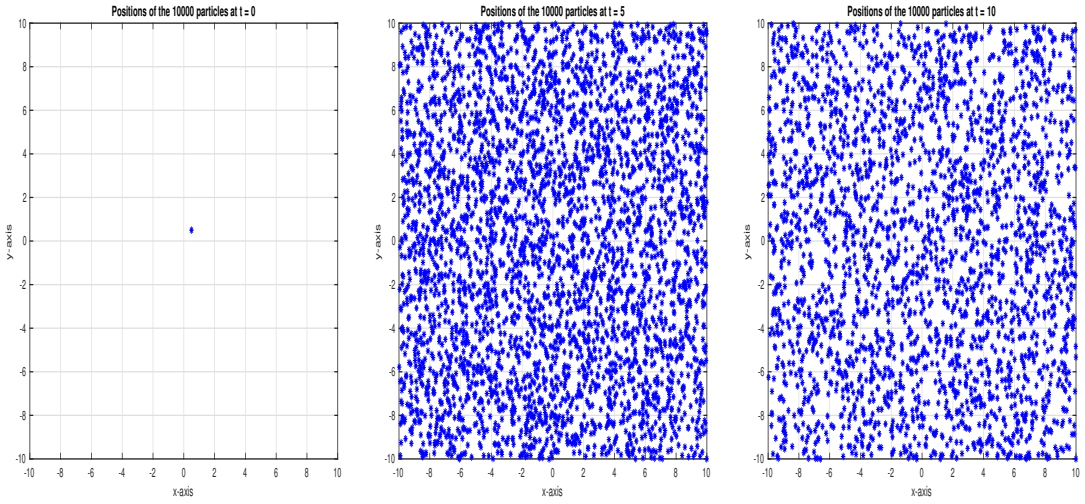

(a) Position of 10 000 particles at t=0

(b) Position of 10 000 particles at t=5

(c) Position of 10 000 particles at t=10

Figure 17: Simulation of particles showing the spread of particles in test environment I

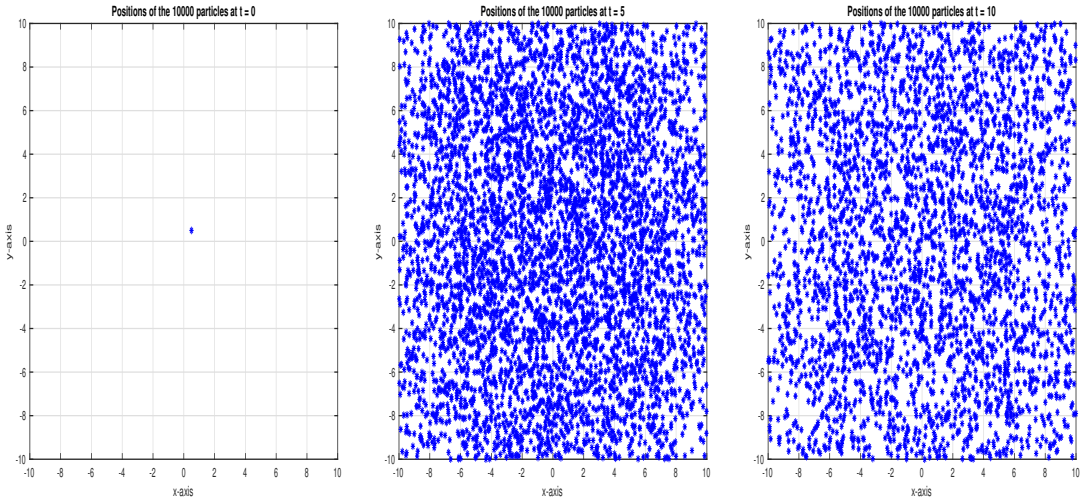

(a) Position of 10 000 particles at t=0

(b) Position of 10 000 particles at t=5

(c) Position of 10 000 particles at t=10

Figure 18: Simulation of particles showing the spread of particles in test environment II

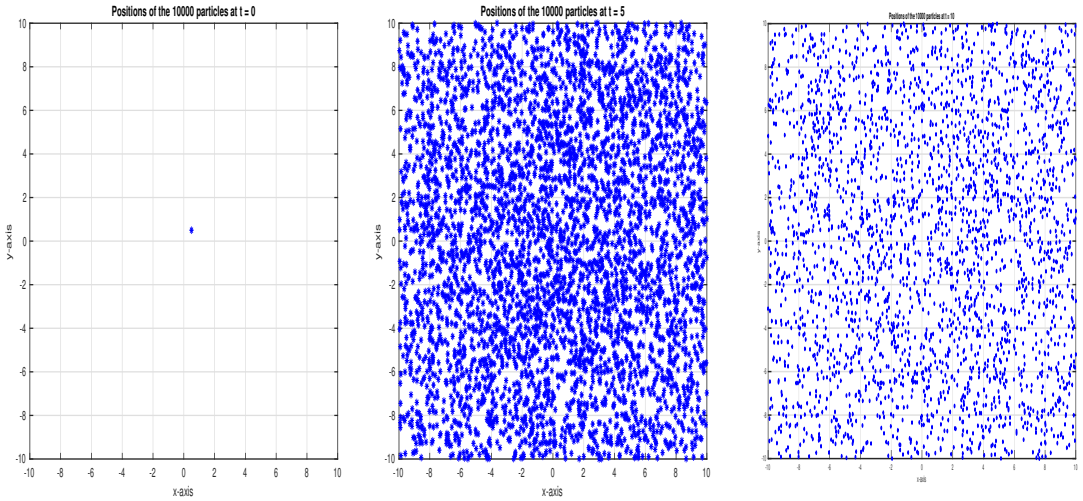

(a) Position of 10 000 particles at t=0

(b) Position of 10 000 particles at t=5

(c) Position of 10 000 particles at t=10

Figure 19: Simulation of particles showing the spread of particles in test environment III

The snapshots obtained through Fig. (17) to Fig. (19) represents distribution of particles when erosion and deposition term are not considered during sediment transport process. Figure 17, 18 and 19 are snapshots for particles distribution in test environment I, II and II respectively. Without inclusion of deposition and erosion terms to the model, it is not possible to record which particles are in suspension or deposited. As a result the distribution of particles obtaiend

through Fig. (17) to Fig. (19) shows that, regardless the change in time the number of particles remained in suspension is the same throught the process. These kind of models assumes there is no deposition of particle as it can be observed that, the number of deposited particles is zero in all test environments. Behaviours of the particles distribution in this case are the same similar to those seen in Test environment I-III in section (4.2). Thus, to have accurate prediction of particles distribution it is very important to put into consideration erosion and deposition terms as it has been considered in this work in which the erosion term is considered as constant and deposition term as a variable.

Table 2: Parameters used in particle model to simulate sediment particle distribution

Constant	Unit	Value
Water viscosity (υ)	-	$1\times2\times10^{-6}$
Water density (ρ_w)	kg/m^3	1000
Gravity of acceleration (g)	m/s^2	9.81
Particle density (ρ_s)	kg/m^3	2650
Sediment diameter (d)	m	0.008
Flow velocity along x-direction (U)	m/s	3
Flow velocity along y-direction (V)	m/s	2.5
Dispersion coefficient (K)	m^2/s	0.01

CHAPTER FIVE

CONCLUSION AND RECOMMENDATIONS

5.1 Conclusion

In this thesis, the particle model were developed through showing consistence relationship between the Fokker-Plank equation and Eulerian sediment transport equation. The model were modified by taking into account erosion term as a constant and deposition term as the function of diffusion coefficient and settling velocity of sediment. The effect of erosion and deposition were also taken into account during the transportation process. Moreover, simulation of the model developed were done by considering three test environments. The effect of each test environment to particles distribution during sediment transport process were analyzed and the corresponding (expected) effects were obtained especially for large value of t. Furthemore, the comparison between the model developed and other models developed without erosion and deposition term were taken into account and effectiveness of the model developed were discussed.

5.2 Recommendations

The study found out that, there is uniformly distribution of sediment particles in Test environment I and III and a linear dependence between the sediment particles and depth in test environment II. Thus through this interesting effect observed in test environment II, this study recommend that in order to mitigate challenges associated with accumulation of sediment particles in ports and harbors, it is very important to take into account depth of the area before construction of Ports and Harbors. In the follow-up research, the expectation is to take a carefully study on Dar es salaam ports and harbors and perform simulation by considering a more realistic domain and other conditions so as to observe more interesting effects as real world phenomena requires realistic condition, Obtain data that will be sufficient enough to simulate bedlevel change and hence to determine the effect of change in water depth. It would also be of interest to take into account the effect of particles with different masses as mass of particle affect deposition and suspension of particle, heavier particles will be faster deposited compared to light one. In this work all particles considered to have the equal mass.

REFERENCES

Amoudry, L. O. and Souza, A. J. (2011). Deterministic coastal morphological and sediment transport modeling: A review and discussion. *Reviews of Geophysics*. **49**(2).

Bakker, S. A. (2009). Uncertainty analysis of the mud infill prediction of the olokola lng terminal. *Ecological Monographs*. **79**(1): 77–108.

Bijker, E. (1980). Sedimentation in channels and trenches. *In:* Coastal Engineering. pp. 1708–1718. https://ascelibrary.org/doi/pdf/10.1061/9780872622647.104.

Björk, T. (2009). Arbitrage theory in continuous time. Oxford university press.

Campolieti, G. and Makarov, R. N. (2018). Financial mathematics: A comprehensive treatment. Chapman and Hall/CRC.

Dade, W. B. and Friend, P. F. (1998). Grain-size, sediment-transport regime, and channel slope in alluvial rivers. *The Journal of Geology*. **106**(6): 661–676.

Dimou, K. N. and Adams, E. E. (1993). A random-walk, particle tracking model for well-mixed estuaries and coastal waters. *Estuarine, Coastal and Shelf Science*. **37**(1): 99–110.

Einstein, H. (1937). Bedload transport as a probability problem. *Sedimentation*. **1027**: C1–C105.

Einstein, H. A. (1950). The bed-load function for sediment transportation in open channel flows. Technical report.

Garrabou, J. and Flos, J. (1995). A simple diffusion-sedimentation model to explain planktonic gradients within a nw mediterranean submarine cave. *Marine Ecology Progress Series*. **123**: 273–280.

Heemink, A. (1990). Stochastic modelling of dispersion in shallow water. *Stochastic hydrology and hydraulics*. **4**(2): 161–174.

Herrera-Díaz, I. E., Torres-Bejarano, F. M., Moreno-Martínez, J. Y., Rodriguez-Cuevas, C. and Couder-Castañeda, C. (2017). Light particle tracking model for simulating bed sediment transport load in river areas. *Mathematical Problems in Engineering*. **2017**.

Higham, D. J. (2001). An algorithmic introduction to numerical simulation of stochastic differential equations. *SIAM review*. **43**(3): 525–546.

Hung, C. S. and Shen, H. W. (1976). Stochastic models of sediment model on flat bed. *Journal of the Hydraulics Division*. **102**(ASCE# 12639).

Jentzen, A. and Kloeden, P. E. (2011). Taylor approximations for stochastic partial differential equations. Vol. 83. SIAM.

Kalinske, A. (1947). Movement of sediment as bed load in rivers. *Eos, Transactions American Geophysical Union*. **28**(4): 615–620.

Kloeden, P. E. and Platen, E. (2013). Numerical solution of stochastic differential equations. Vol. 23. Springer Science & Business Media.

Knaapen, M. A. and Wertwijn, C. (2013). Probabilistic channel infill approach. In: *XXth TELEMAC-MASCARET. User Conference 2013*. pp. 99–102.

Li, R.-M. and Shen, H. W. (1975). Solid particle settlement in open-channel flow. *Journal of the Hydraulics Division*. **101**(ASCE# 11460 Proceeding).

Mahera, W. and Narsis, A. (2013). Modelling of sediment transport in shallow waters modelling of sediment transport in shallow waters by by stochastic and partial differential equations stochastic and partial differential equations. *IntechOpen*. pp. 309–328.

Man, C. and Tsai, C. W. (2007). Stochastic partial differential equation-based model for suspended sediment transport in surface water flows. *Journal of engineering mechanics*. **133**(4): 422–430.

Milstein, G. N. (1994). Numerical integration of stochastic differential equations. Vol. 313. Springer Science & Business Media.

Oh, J. and Tsai, C. W. (2010). A stochastic jump diffusion particle-tracking model (sjd-ptm) for sediment transport in open channel flows. *Water Resources Research*. **46**(10).

Øksendal, B. (2003). Stochastic differential equations. *In:* Stochastic differential equations. Springer. pp. 65–84.

Prickett, T. A., Lonnquist, C. G., Naymik, T. G. *et al.* (1981). A" random-walk" solute transport model for selected groundwater quality evaluations. *Bulletin (Illinois State Water Survey) no. 65*. .

Rijn, L. C. v. (1986). Sedimentation of dredged channels by currents and waves. *Journal of Waterway, Port, Coastal, and Ocean Engineering*. **112**(5): 541–559.

Sanga, I. and Dubi, A. (2004). Impact of improvement of the entrance channel on the rate of sediment deposition into the dar es salaam harbour. *Western Indian Ocean Journal of Marine Science*. **3**(2): 105–112.

Schuttelaars, H. and De Swart, H. (1997). An idealized long-term morphodynamic model of a tidal embayment. . .

Senior, A., Green, M. and Oldman, J. (2003). Using deterministic models to assess risk in sediment-impacted estuaries. *In:* The Interactions between Sediments and Water. Springer. pp. 11–16.

Uffink, G. (1983). A random walk method for the simulation of macrodispersion in a stratified aquifer. *Relation of groundwater quantity and quality*. pp. 103–114.

Union, A. G. (1957). Sediment classification system.

Van Rijn, L. C. *et al.* (1990). Principles of fluid flow and surface waves in rivers, estuaries, seas and oceans. Vol. 12. Aqua Publications Amsterdam.

Zhao, J., Özgen-Xian, I., Liang, D., Wang, T. and Hinkelmann, R. (2019). A depth-averaged non-cohesive sediment transport model with improved discretization of flux and source terms. *Journal of hydrology*. **570**: 647–665.

APPENDICES

Appendix I: MATLAB codes

%MATLAB code for figure 2.

```
randn('state',100)
T = 1; N = 700; dt = T/N;
dW = zeros(1,N);
W = zeros(1,N);
dW(1) = sqrt(dt)*randn;
W(1) = dW(1);
for j = 2:N
   dW(j) = sqrt(dt)*randn;
   W(j) = W(j-1) + dW(j);
end
plot([0:dt:T],[0,W],'g-')
xlabel('t','FontSize',16)
ylabel('W(t)','FontSize',16,'Rotation',0)
```

% MATLAB code for figure 3.

```
randn('state',100)
lambda = 2; mu = 1; Xzero = 1;
T = 1; N = 2^8; dt = 1/N;
dW = sqrt(dt)*randn(1,N);
W = cumsum(dW);
% problem parameters
% Brownian increments
% discretized Brownian path
Xtrue = Xzero*exp((lambda-0.5*mu^2)*([dt:dt:T])+mu*W);
plot([0:dt:T],[Xzero,Xtrue],'m-'), hold on
R = 4; Dt = R*dt; L = N/R;         % L EM steps of size Dt = R*dt
Xem = zeros(1,L);                  % preallocate for efficiency
Xtemp = Xzero;
for j = 1:L
   Winc = sum(dW(R*(j-1)+1:R*j));
   Xtemp = Xtemp + Dt*lambda*Xtemp + mu*Xtemp*Winc;
   Xem(j) = Xtemp;
end
plot([0:Dt:T],[Xzero,Xem],'b--*'), hold off
xlabel('t','FontSize',12)
ylabel('X','FontSize',16,'Rotation',0,'HorizontalAlignment','right')
legend('Exact Solution','Euler Approximated solution')
emerr = abs(Xem(end)-Xtrue(end))
```

% MATLAB code for figure 4.

```
[x,y]=meshgrid(-10:1:10);
z=10+10.*exp(-0.03.*(x.^2+y.^2));
surf(x,y,z),xlabel('x-axis'),ylabel('y-axis'),zlabel('Dispersion
coefficient')
```

% MATLAB code for figure 5-8.

```
clf;
```

```
clear
close all
n = 10000;
ndep=0;
x = zeros(1,n)+0.5;
y = zeros(1,n)+0.5;
dx = zeros(1,n);
dy = zeros(1,n);
r = 0.2;
%U =cos((pi*x)/20).*sin((pi*y)/20) ;
%V = -sin((pi*x)/20).*cos((pi*y)/20);
p=1;
%a=0.1;
vis=1.2*10^-6;
d=0.008;
seddens=2650;
watdens=1000;
g=9.81;
D=1.25;
b=sqrt((13.95*(vis/d))^2+1.09*(seddens/watdens-1)*g*d)-13.95*(vis/d);
a=(b^2/D);
tStart = 0;
tEnd   = 10;
steps  = 10;
%disp('=========================================             ')
%disp(['tStart='num2str(tStart) 'p='num2str(p)  'n= ' num2str(n)])
t = linspace(tStart, tEnd, steps+1);
dt = t(2) - t(1);

xdeposited = 0;
ydeposited = 0;

for i=1:steps+1
                                    %flushes the event queue" and forces
MATLAB to update the screen.
          %hold on;
    %%quiver(x,y,dx,dy),axis([-21 21 -21 21]),grid on;
    figure
     %clf;
    subplot(2,2,1);
    plot(x,y,'b*');
    %axis([-10000 12500 -10000 12500]),grid on,box on,
    %axis([-20.50 21 -20.50 21]),grid on,box on,
    axis([-10 10 -10 10]),grid on,box on,
    title(['Positions of the', ' ', num2str(n), ' ', 'suspended particles at
t =', ' ', num2str((i-1)*dt)])
    xlabel('x-axis');
    ylabel('y-axis');
    %axis('auto')

    %%%%%%%%%%%%% .  deposited plot . %%%%%%%%%%%%%%%%
    subplot(2,2,2);
    scatter(xdeposited, ydeposited, '.')
    axis([-10 10 -10 10]),grid on,box on
title(['Positions of the', ' ', num2str(ndep), ' ', 'deposited particles at t
=', ' ', num2str((i-1)*dt)])
    xlabel('x-axis');
    ylabel('y-axis');
```

```
    %%%%%%%%%%%% histogram %%%%%%%%%%%%%%
    edgeLimit = 6;
    binWidth = 0.3;
    edge1dim = -edgeLimit:binWidth:edgeLimit;
    edges = {edge1dim, edge1dim};
    Xdeposited = [xdeposited', ydeposited'];

    subplot(2,2,3);
    hist3(Xdeposited, 'Edges', edges)
    title(['Histogram of the', ' ', num2str(ndep), ' ', 'deposited particles
at t =', ' ', num2str((i-1)*dt)])
    xlabel('x-axis');
    ylabel('y-axis');

    drawnow;

    if (i < steps)
        if (n == 0) break; end
        H=10;
        dHdx=0;
        dHdy=0;
        U = 3;
        V = 2.5;
        D=exp((-x).^2+(y).^2)/(2*r^2);
        dDdx = -20*x .* sin((x.^2+y.^2)*4);
        dDdy = -20*y .* sin((x.^2+y.^2)*4);
        dx = (U + dHdx.*D./H + dDdx);
        dy = (V + dHdy.*D./H + dDdy);
        % x = x + (U + dHdx.*D./H + dDdx) * dt + sqrt(2*3*D*dt).*rand(1,n);
        %y = y + (V + dHdy.*D./H + dDdy) * dt + sqrt(2*3*D*dt).*rand(1,n);
%        te=x(1)
        x = x + (U + dHdx.*D./H + dDdx) * dt +
sqrt(2*D*dt).*((rand(1,n)*sqrt(12))-sqrt(3));
%        ten=x(1)
%        figure(33)
%        plot([i i+1],[te ten])
%        hold on
        y = y + (V + dHdy.*D./H + dDdy) * dt +
sqrt(2*D*dt).*((rand(1,n)*sqrt(12))-sqrt(3));
        % This part is expected to compute the probability part of the
particle

        pnew=p.*(1-a*dt)                                % calculates the new
probability that the particle will be killed.
        tem=rand(1,n);                                    % the random numbers
that help to determine  which particles have been killed
        nnew=length(find(tem<pnew));                     % this gives the
number of new particles that have remained in the flow
        xdeposited = [xdeposited, x(tem>=pnew)];
        ydeposited = [ydeposited, y(tem>=pnew)];

        x = x(find(tem<pnew));
y = y(find(tem<pnew));                              %  finds the location (x,y)
of the remaining particles in the flow  and use them in the loop.
          %disp(['t=' num2str(t) 'p=' num2str(pnew) 'n=' num2str(nnew)])
        p=pnew;
```

```
        n=nnew;
        ndep=10000-n;
        pause(0.5);                                                %pauses for
0.2 seconds before continuing
        %  pause;
        %function [D] = diffusion(x, y)

%end% causes a procedure to stop and wait for the user to strike any key
before continuing.

    end;

    end;
%     r=3;
%     N=20;
%     P=1-1/(U^2+V^2)^r
%     particle=rand(1,N);
%     ncreated=length(find(particle<P));
%    palive=[palive,ones(1,ncreated)];
%     %xcreated=[palive,ones(1,ncreated)];
%     %xcreated=[palive,ones(1,ncreated)];
%     xcreated=ncreated;
%     ycreated=ncreated;
%     x=[x,xcreated];
%     y=[y,xcreated];
%      n=size(x,2);
%      figure(44)
%      plot(x,y,'r*',xcreated,ycreated,'b*'),grid on;
%      title(num2str(ncreated))
%
```

% MATLAB code for figure 9 .

```
[x,y]=meshgrid(-10:.1:10);
z=10-5.*tanh(x-4)+5.*tanh(x+4);
surf(x,y,z),xlabel('x-axis'),ylabel('y-axis'),zlabel('Space varying depth')
```

% MATLAB code for figure 10-13 .

```
clf;
clear
close all
n = 10000;
ndep=0;
x = zeros(1,n)+0.5;
y = zeros(1,n)+0.5;
dx = zeros(1,n);
dy = zeros(1,n);
r = 0.2;
%U =cos((pi*x)/20).*sin((pi*y)/20) ;
%V = -sin((pi*x)/20).*cos((pi*y)/20);
p=1;
%a=0.1;
vis=1.2*10^-6;
d=0.008;
seddens=2650;
watdens=1000;
g=9.81;
```

```
D=1.25;
b=sqrt((13.95*(vis/d))^2+1.09*(seddens/watdens-1)*g*d)-13.95*(vis/d);
a=(b^2/D);
tStart = 0;
tEnd   = 10;
steps  = 10;
%disp('=========================================            ')
%disp(['tStart='num2str(tStart) 'p='num2str(p)  'n= ' num2str(n)])
t = linspace(tStart, tEnd, steps+1);
dt = t(2) - t(1);

xdeposited = 0;
ydeposited = 0;

for i=1:steps+1
                                    %flushes the event queue" and forces
MATLAB to update the screen.
          %hold on;
    %%quiver(x,y,dx,dy),axis([-21 21 -21 21]),grid on;
    figure
     %clf;
    subplot(2,2,1);
    plot(x,y,'b*');
    %axis([-10000 12500 -10000 12500]),grid on,box on,
    %axis([-20.50 21 -20.50 21]),grid on,box on,
    axis([-10 10 -10 10]),grid on,box on,
    title(['Positions of the', ' ', num2str(n), ' ', 'suspended particles at
t =', ' ', num2str((i-1)*dt)])
    xlabel('x-axis');
    ylabel('y-axis');
    %axis('auto')

    %%%%%%%%%%%%%% .  deposited plot . %%%%%%%%%%%%%%%%%
    subplot(2,2,2);
    scatter(xdeposited, ydeposited, '.')
    axis([-10 10 -10 10]),grid on,box on
    title(['Positions of the', ' ', num2str(ndep), ' ', 'deposited particles
at t =', ' ', num2str((i-1)*dt)])
    xlabel('x-axis');
    ylabel('y-axis');

    %%%%%%%%%%%%% histogram %%%%%%%%%%%%%%%
    edgeLimit = 6;
    binWidth = 0.3;
    edge1dim = -edgeLimit:binWidth:edgeLimit;
    edges = {edge1dim, edge1dim};
    Xdeposited = [xdeposited', ydeposited'];

    subplot(2,2,3);
    hist3(Xdeposited, 'Edges', edges)
    title(['Histogram of the', ' ', num2str(ndep), ' ', 'deposited particles
at t =', ' ', num2str((i-1)*dt)])
    xlabel('x-axis');
    ylabel('y-axis');

    drawnow;
```

```
    if (i < steps)
        if (n == 0) break;
        H    = 10-5*tanh(x-4)+5*tanh(x+4);
        dHdx=-5*(sech(x - 4)).^2+5*(sech(x+ 4)).^2;
        dHdy=0;
        U = 3;
        V = 2.5;
        D = 10;
        dDdx=0;
        dDdy=0;
        dx = (U + dHdx.*D./H + dDdx);
        dy = (V + dHdy.*D./H + dDdy);
        % x = x + (U + dHdx.*D./H + dDdx) * dt + sqrt(2*3*D*dt).*rand(1,n);
        %y = y + (V + dHdy.*D./H + dDdy) * dt + sqrt(2*3*D*dt).*rand(1,n);
%        te=x(1)
        x = x + (U + dHdx.*D./H + dDdx) * dt +
sqrt(2*D*dt).*((rand(1,n)*sqrt(12))-sqrt(3));
%        ten=x(1)
%        figure(33)
%        plot([i i+1],[te ten])
%        hold on
        y = y + (V + dHdy.*D./H + dDdy) * dt +
sqrt(2*D*dt).*((rand(1,n)*sqrt(12))-sqrt(3));
        % This part is expected to compute the probability part of the
particle

        pnew=p.*(1-a*dt)                                % calculates the new
probability that the particle will be killed.
        tem=rand(1,n);                                    % the random numbers
that help to determine  which particles have been killed
        nnew=length(find(tem<pnew));                     % this gives the
number of new particles that have remained in the flow
        xdeposited = [xdeposited, x(tem>=pnew)];
        ydeposited = [ydeposited, y(tem>=pnew)];

        x = x(find(tem<pnew));
        y = y(find(tem<pnew));                             %  finds the
location (x,y) of the remaining particles in the flow  and use them in the
loop.
          %disp(['t=' num2str(t) 'p=' num2str(pnew) 'n=' num2str(nnew)])
        p=pnew;
        n=nnew;
        ndep=10000-n;
        pause(0.5);                                                %pauses for
0.2 seconds before continuing
        %  pause;
%function [D] = diffusion(x, y)

%end% causes a procedure to stop and wait for the user to strike any key
before continuing.

    end;

    end;
%     r=3;
%     N=20;
%     P=1-1/(U^2+V^2)^r
```

```
%     particle=rand(1,N);
%     ncreated=length(find(particle<P));
%    palive=[palive,ones(1,ncreated)];
%     %xcreated=[palive,ones(1,ncreated)];
%     %xcreated=[palive,ones(1,ncreated)];
%     xcreated=ncreated;
%     ycreated=ncreated;
%     x=[x,xcreated];
%     y=[y,xcreated];
%      n=size(x,2);
%      figure(44)
%      plot(x,y,'r*',xcreated,ycreated,'b*'),grid on;
%      title(num2str(ncreated))
%
```

% MATLAB code for figure 14 .

```
[x,y]=meshgrid(-10:.8:10,-10:.8:10);
u=cos((pi*x)/20).*sin((pi.*y)/20);
v=-sin((pi*x)/20).*cos((pi.*y)/20);
X1 = [-10,0,10];
Y1 = [0,0,0];
X2 = [0,0,0];
Y2 = [-10,0,10];
figure
plot(X1,Y1,'r')
hold on
plot(X2,Y2,'r')
hold on
quiver(x,y,u,v)
hold off
```

%Matlab code for figure 15-16.

```
clf;
clear
close all
n = 10000;
ndep=0;
x = zeros(1,n)+0.5;
y = zeros(1,n)+0.5;
dx = zeros(1,n);
dy = zeros(1,n);
r = 0.2;
%U =cos((pi*x)/20).*sin((pi*y)/20) ;
%V = -sin((pi*x)/20).*cos((pi*y)/20);
p=1;
%a=0.1;
vis=1.2*10^-6;
d=0.008;
seddens=2650;
watdens=1000;
g=9.81;
D=1.25;
b=sqrt((13.95*(vis/d))^2+1.09*(seddens/watdens-1)*g*d)-13.95*(vis/d);
a=(b^2/D);
tStart = 0;
```

```
tEnd   = 10;
steps  = 10;
%disp('=========================================             ')
%disp(['tStart='num2str(tStart) 'p='num2str(p)  'n= ' num2str(n)])
t = linspace(tStart, tEnd, steps+1);
dt = t(2) - t(1);

xdeposited = 0;
ydeposited = 0;

for i=1:steps+1
                                    %flushes the event queue" and forces
MATLAB to update the screen.
          %hold on;
    %%quiver(x,y,dx,dy),axis([-21 21 -21 21]),grid on;
    figure
     %clf;
    subplot(2,2,1);
    plot(x,y,'b*');
    %axis([-10000 12500 -10000 12500]),grid on,box on,
    %axis([-20.50 21 -20.50 21]),grid on,box on,
    axis([-10 10 -10 10]),grid on,box on,
    title(['Positions of the', ' ', num2str(n), ' ', 'suspended particles at
t =', ' ', num2str((i-1)*dt)])
    xlabel('x-axis');
    ylabel('y-axis');
    %axis('auto')

    %%%%%%%%%%%%% .  deposited plot . %%%%%%%%%%%%%%%%
    subplot(2,2,2);
    scatter(xdeposited, ydeposited, '.')
    axis([-10 10 -10 10]),grid on,box on
    title(['Positions of the', ' ', num2str(ndep), ' ', 'deposited particles
at t =', ' ', num2str((i-1)*dt)])
    xlabel('x-axis');
    ylabel('y-axis');

    %%%%%%%%%%%% histogram %%%%%%%%%%%%%
    edgeLimit = 6;
    binWidth = 0.3;
    edge1dim = -edgeLimit:binWidth:edgeLimit;
    edges = {edge1dim, edge1dim};
    Xdeposited = [xdeposited', ydeposited'];

    subplot(2,2,3);
hist3(Xdeposited, 'Edges', edges)
title(['Histogram of the', ' ', num2str(ndep), ' ', 'deposited particles at t
=', ' ', num2str((i-1)*dt)])
    xlabel('x-axis');
    ylabel('y-axis');

    drawnow;

    if (i < steps)
        if (n == 0) break; end
        U = cos((pi*x)/20).*sin((pi*y)/20) ;
        V = -sin((pi*x)/20).*cos((pi*y)/20);
```

```
        H=10;
        dHdx=0;
        dHdy=0;
        D = 10;
        dDdx=0;
        dDdy=0;
        dx = (U + dHdx.*D./H + dDdx);
        dy = (V + dHdy.*D./H + dDdy);
        % x = x + (U + dHdx.*D./H + dDdx) * dt + sqrt(2*3*D*dt).*rand(1,n);
        %y = y + (V + dHdy.*D./H + dDdy) * dt + sqrt(2*3*D*dt).*rand(1,n);
%        te=x(1)
        x = x + (U + dHdx.*D./H + dDdx) * dt +
sqrt(2*D*dt).*((rand(1,n)*sqrt(12))-sqrt(3));
%        ten=x(1)
%        figure(33)
%        plot([i i+1],[te ten])
%        hold on
        y = y + (V + dHdy.*D./H + dDdy) * dt +
sqrt(2*D*dt).*((rand(1,n)*sqrt(12))-sqrt(3));
        % This part is expected to compute the probability part of the
particle

        pnew=p.*(1-a*dt)                                % calculates the new
probability that the particle will be killed.
        tem=rand(1,n);                                    % the random numbers
that help to determine  which particles have been killed
        nnew=length(find(tem<pnew));                    % this gives the
number of new particles that have remained in the flow
        xdeposited = [xdeposited, x(tem>=pnew)];
        ydeposited = [ydeposited, y(tem>=pnew)];

        x = x(find(tem<pnew));
        y = y(find(tem<pnew));                              %  finds the
location (x,y) of the remaining particles in the flow  and use them in the
loop.
          %disp(['t=' num2str(t) 'p=' num2str(pnew) 'n=' num2str(nnew)])
        p=pnew;
        n=nnew;
        ndep=10000-n;
        pause(0.5);                                                 %pauses for
0.2 seconds before continuing
        %  pause;
        %function [D] = diffusion(x, y)

%end% causes a procedure to stop and wait for the user to strike any key
before continuing.

    end;

    end;
```